

## The premelting of ice and its environmental consequences

J G Dash†, Haiying Fu† and J S Wettlaufer‡

†Department of Physics, MS FM-15, University of Washington, Seattle, Washington 98195, USA

‡Applied Physics Laboratory, MS HN-10, University of Washington, Seattle, Washington 98195, USA

### Abstract

Several mechanisms can extend the equilibrium domain of a liquid phase into the solid region of the normal phase diagram. The causes of *premelting*, which include surface melting, interface curvature and substrate disorder, occur in all types of substances, including H<sub>2</sub>O. In the case of H<sub>2</sub>O, premelting can have important environmental consequences, among which are the heaving of frozen ground, breakdown of rock and concrete, sintering of snow, flow of glaciers, scavenging of atmospheric trace gases by snow and ice, and the electrification of thunderclouds. This article reviews the basic mechanisms of premelting and discusses their roles in the environmental phenomena. The principal results of numerous studies are reviewed, and trends in current research are outlined.

This review was received in June 1994.

**Contents**

	Page
1. Introduction	117
1.1. History, confusion and debate: regelation, friction and frost heave	117
1.2. Brief description of some environmental effects	118
2. Physics of premelting	118
2.1. Surface melting	118
2.2. Interfacial and grain boundary melting	126
2.3. Size effects in premelting	128
2.4. Surface disorder	129
2.5. Supercooling, stability and nucleation	130
2.6. Solutes: solid–liquid distribution	133
3. Premelting of ice. Laboratory studies	135
3.1. Vapour interfaces	135
3.2. Interfacial melting at solid walls	137
3.3. Crystal growth	138
4. Non-equilibrium effects: thermomolecular pressure and transport	140
5. Ice in the environment	142
5.1. Friction; ice and snow	144
5.2. Soil freezing, permafrost and frost heave	146
5.3. Glaciers, sea ice and snow fields; sintering and sliding	152
5.4. Atmospheric ice	157
Acknowledgments	159
References	159

## 1. Introduction

The phenomena treated in this review touch virtually every portion of the globe and most of its inhabitants. They range from the commonplace—the slipperiness of ice and snow—to the less well known and still controversial—the mechanism of charging of thunderclouds and the destruction of ozone in polar atmospheres. Yet such greatly different effects originate in a small set of related basic processes: surface and size effects in the melting transition of ice. They all involve *premelting*, which is the existence of liquid at temperatures and pressures below the normal phase boundary. Premelting can be caused by several mechanisms, including static and dynamic, chemical, mechanical, interfacial and structural processes. The basic mechanisms are not unique to ice; they occur in all types of solids. However, they stand out in the case of ice because of the ubiquity and importance of their environmental effects. As a consequence, the ice phenomena have been studied for many years; some of them, for centuries. Yet fundamental questions and practical problems remain today, as demanding as at any time in the past. Consequently, ice is both a challenge and a test bed. In this review we attempt to present a picture of what is known and what is still to be resolved.

### 1.1. History, confusion and debate: regelation, friction and frost heave

On 8 September 1842 Michael Faraday recorded his thoughts about snow and ice, and he then began a series of investigations that were to last twenty years. Excerpts from his diary, published many years later (Faraday 1850, 1933) record the beginning of the first scientific investigation into what we now know as surface melting.

*When wet snow is squeezed together, it freezes into a lump (with water between) and does not fall asunder as so much wetted sand or other kind of matter would do.*

*In a warm day, if two pieces of ice be laid one on the other and wrapped up in flannel, they will freeze into one piece.*

*All this seems to indicate that water at 32° will not continue as water, if it be between two surfaces of ice touching or very near to each other.*

*The ice probably acts as a nucleus, but it appears that the effect of one surface of ice on water is not equal to the joint effect of two.*

Although experiments by Faraday and others (Tyndall 1856) were proof to them of a liquid film at equilibrium, some contemporaries were unconvinced. James Thomson and his brother Sir William Thomson, who later became Lord Kelvin, countered with an explanation growing out of their work on pressure melting. They argued that *regelation* (sintering is the modern term) of ice results from the lowering of the melting temperature due to the temporary increase of pressure at the points of contact, and this came to be the accepted explanation for the rapid sintering and slipperiness of ice. But a simple calculation shows that pressure melting cannot account for the low friction coefficient except at temperatures very close to the normal melting point. The slope of the melting line is about 136 bar K<sup>-1</sup>; for a typical person on a conventional skate, the depression of the melting point is less than 0.1 K.

At lower temperatures, friction on ice involves several distinct surface and thermal phenomena which still merit active research; in spite of its apparent banality, the slipperiness of ice and snow is far from a closed subject.

### *1.2. Brief description of some environmental effects*

The effects of frost heave are familiar to most people living in temperate and colder regions, where roads and other ground-level structures are shifted or deformed during the winter season. To the uninitiated, the stresses seem to be due to the expansion of water when it freezes. But this accounts for only a minor fraction of the stress: the greater part is due to migration of unfrozen water in the ground.

A description of frost heave and its serious consequences is given in a National Research Council report (Polar Research Board 1984):

*Nearly everyone living in the northern and southern temperate zones has experienced the effects of ice segregation and frost heaving through the destruction of roads and highways, the displacement of foundations, the jamming of doors, the misalignment of gates, and the cracking of masonry. Many people often have simply and mistakenly assumed that these effects result solely from the expansion of pore water on freezing. When confined, water can rupture pipes, break bottles, and crack rocks as it freezes. However, most of the destructive effects of frost heaving are caused by 'ice segregation', a complex process that results from the peculiar behavior of water and other liquids as they freeze within porous materials. In particular, water is drawn to the freezing site from elsewhere by the freezing process itself. When this water accumulates as ice, it forces the soil apart, producing expansion of the external soil boundaries, as well as internal consolidation. The dynamic process of ice segregation and the expansion resulting from freezing of the in situ pore water, together, cause frost heaving.*

Beyond its damaging effects on engineered structures, frost heave is one of the major evolutionary mechanisms in the geology of a great fraction of the world's surface. It breaks down the integrity of exposed rock, and speeds its transformation to soil. It causes the churning of the upper layers of the ground, and can produce extensive and regular networks of patterned ground. Figure 1 is a photograph of a prime example of such patterned ground.

In this review we trace the connections from the microscopic mechanisms, some of which are continuing subjects of study, to many familiar and important phenomena in the natural environment.

## **2. Physics of premelting**

There are many mechanisms that can cause the stable existence of liquid at temperatures and pressures outside the normal equilibrium range. These mechanisms are universal, in that they can affect all classes of solids. In this section we review the theory and experimental observations on specific substances, while reserving discussions of effects on ice for a later section.

### *2.1. Surface melting*

The existence of thin liquid-like films on solid surfaces at temperatures below the bulk transition was deduced by Tammann (1910) and Stranski (1942) from the absence of superheating. Frenkel (1946) describes the argument, as follows.

*It is well known that under ordinary conditions an overheating of [a crystal], similar to the overheating of a liquid, is impossible. This peculiarity is connected with the fact that the melting of a crystal, which is kept at a homogeneous temperature, always begins on its free surface. The role of the latter must, accordingly, consist in lowering the activation energy,*



**Figure 1.** Stone circles on Spitzbergen Island (Hallet 1989). Geometric patterns of rocks, soil and ice develop spontaneously in Arctic and alpine soils where the temperature fluctuates about the freezing point. Patterned ground is a particularly striking result of soil motion due to freezing and thawing termed 'cryoturbation'.

*which is necessary for the formation of a flat embryo of the liquid phase, i.e. of a thin liquid film, down to zero.*

Many years after the first deductions of *premelting*, the existence of liquid-like surface films at temperatures below the bulk melting point has been substantiated by experiments on many classes of solids. We now have experimental proof of the phenomenon on surfaces of metals, semiconductors, solid rare gases and molecular solids. The modern theory of surface melting explains the behaviour in considerable detail, and can relate its characteristics to material properties. Typically, surface melting begins with one or two monolayers' thickness at  $T < 0.9$  of the bulk melting temperature  $T_0$ , thickens gradually with increasing  $T$ , and diverges at  $T_0$ . The effect is driven by the tendency to reduce the interfacial free energy. Variants of surface melting include grain boundary melting (premelting at junctions between crystals of the same material) and interfacial melting (premelting at boundaries with foreign solids).

Recent reviews of surface melting have been published by van der Veen *et al* (1988),

Dash (1989a, 1991), Chernov (1993a) and Löwen (1994).

**2.1.1. Theory.** If the interface between a solid and its vapour is wetted by the liquid phase (meaning that a layer of the liquid phase intervenes between the solid and the vapour), it implies that the free energy of the wetted boundary is lower than it would be without the liquid. We can also infer that a wetting layer will persist over some finite temperature range below the normal melting point. For, if the state of the system slightly below the bulk melting temperature were to be initially dry, the system could lower its free energy by converting a layer of the solid to liquid. The cost of this conversion involves the free energy change due to melting, but if the layer is thin enough and the temperature sufficiently close to the bulk melting point the cost will not be prohibitive. This competition between surface and conversion terms establishes the actual thickness of the liquid: it is the value at which the free energy of the *system* is a minimum. The theoretical thickness-temperature relation and its dependence on the nature of the molecular interactions are derived as follows.

Consider a solid in equilibrium with a vapour at temperature  $T$  and pressure  $P$ . If the interface is wetted by a macroscopic layer of the pure melt (m) liquid, the free energy of the layer is composed of bulk and surface terms. The free energy per unit area can be written as

$$G_m(T, P, d) = [\rho_l \mu_l(T, P)]d + \gamma(d) \quad (2.1)$$

where  $d$  is the thickness,  $\rho_l$  and  $\mu_l$  are the density and chemical potential of the bulk liquid (l), and  $\gamma(d)$  is the interfacial coefficient. Its value varies from  $\gamma_{sv}$ , the coefficient of the unwetted solid-vapour interface, at  $d = 0$ , to  $\gamma_v + \gamma_s$  at  $d = \infty$ . Its functional dependence on  $d$  reflects the type of basic interactions in the material. To bring out the variation more explicitly, we write

$$\gamma(d) = \Delta\gamma f(d) + \gamma_{sv} \quad (2.2)$$

where

$$\Delta\gamma \equiv \gamma_v + \gamma_s - \gamma_{sv}. \quad (2.3)$$

The interfacial potential  $f(d)$  ranges from 0 to 1 as  $d$  increases from 0 to  $\infty$ .

In thermodynamic equilibrium, the chemical potential of the melted layer is equal to that of the solid. Substituting equations (2.2) and (2.3) in equation (2.1) and differentiating with respect to  $d$  yields

$$\mu_m(T, P, d) = \frac{1}{\rho_l} \left( \frac{\partial G_m}{\partial d} \right)_{T, P} = \mu_l(T, P) + \left( \frac{\Delta\gamma}{\rho_l} \right) \frac{\partial f}{\partial d} = \mu_s(T, P). \quad (2.4)$$

The interfacial term in equation (2.4) introduces a difference between the chemical potentials of the solid and liquid, which displaces the location of the thermodynamic coordinates from the normal phase boundary. The displacement can be calculated by a series expansion of the chemical potential in powers of temperature and pressure about the normal bulk position  $T_0$ ,  $P_0$ . To first order,

$$\begin{aligned} \Delta\mu(T, P) &= \left[ \frac{\partial \Delta\mu}{\partial T} \right]_{T_0} (T - T_0) + \left[ \frac{\partial \Delta\mu}{\partial P} \right]_{P_0} (P_s - P_0) \\ &= \frac{g_m}{T_0} (T - T_0) - \left( \frac{1}{\rho_l} - \frac{1}{\rho_s} \right) (P_s - P_0) \end{aligned} \quad (2.5)$$

where  $\Delta\mu \equiv \mu_s - \mu_l$ , and  $q_m$  is the latent heat of melting per molecule. The pressure shift can be expressed in terms of the temperature shift and the slopes of the sublimation and melting lines, through the Clausius–Clapeyron relation. Equation (2.5) can then be transformed to

$$\Delta\mu = \kappa_v q_m (T - T_0) / T_0 \quad (2.6)$$

where

$$\kappa_v = \left[ 1 - (\mathrm{d}P/\mathrm{d}T)_{sv} / (\mathrm{d}P/\mathrm{d}T)_{sl} \right]. \quad (2.7)$$

The pressure term in equation (2.7) is typically a minor contribution; in H<sub>2</sub>O, for example,  $\kappa_v$  differs from unity by about 3 ppm.

Equation (2.6), together with the specific interfacial potential  $f(d)$ , leads to the theoretical expression for thickness. In typical molecular substances with unretarded dispersion or van der Waals forces, the long-range potentials fall off quadratically with distance. The interfacial potential has the form

$$f(d) = d^2 / (d^2 + \sigma^2) \quad (2.8)$$

where  $\sigma$  is a constant on the order of a molecular diameter. In this case, a combination of equations (2.4), (2.6) and (2.8) in the range  $d \gg \sigma$  leads to

$$d = \left( -2\sigma^2 \frac{\Delta\gamma}{\rho_l q_m} \right)^{1/3} t^{-1/3} \quad (2.9)$$

where  $t$  is the reduced temperature  $(T_0 - T) / T_0$ . In the case of short-range forces,

$$\partial f / \partial d \propto \exp(-cd) \quad (2.10)$$

where  $c$  is a constant. The thickness then varies logarithmically with temperature,

$$d \propto |\ln t|. \quad (2.11)$$

Other interactions, such as dipolar forces, can produce other similarly specific temperature dependences.

**2.1.2. Surface melting observations (excepting ice).** The principal results of the thermodynamic description in section 2.1.1 are confirmed by experiments and computer simulations. In addition, several important features that are neglected in the simple model have been seen in laboratory studies, computations and more detailed theories, as summarized below.

**Melting is initiated at the surface.** The first clear microscopic evidence of surface melting was seen by ion backscattering from the (100) plane of lead (Frenken and van der Veen 1985). In this technique, the intensity of 1–10 keV proton beams is measured at specific incident and detection ‘blocking’ angles, where scattering in the backward direction is prevented by the regular rows of atoms. However, surface disorder allows scattering into the blocked direction, and hence is indicated by a rise in intensity. Other direct surface measurements have been made by x-rays (Fuoss *et al* 1988), low-energy electron diffraction

(Prince *et al* 1988), neutron diffraction (Krim *et al* 1987), quasi-elastic neutron scattering (Zeppenfeld *et al* 1990) and He atom scattering (Frenken *et al* 1988). Computer simulations have shown greater detail; layer by layer melting, beginning at the vapour interface, of argon (Valkealahti and Nieminen 1987, Phillips 1990) and methane films (Phillips 1989, 1990) and close-packed metals Au (Carnevali *et al* 1987) and Cu (Häkkinen and Manninen 1992, Häkkinen and Landman 1993).

The reason that melting begins at the surface is the weaker binding and anharmonicity of the outermost atoms, which cause an instability of the surface atoms before the deeper atoms (Pietronero and Tosatti 1979).

*Surface melting is an equilibrium phenomenon.* The proof that the quasi-liquid film is stable comes from many of the experiments and computer simulations quoted above. In addition to these studies, there have been several calorimetric studies of thin adsorbed films, in which premelting causes a significant precursor in the specific heat below the bulk transition (Zhu and Dash 1986). Such studies give reproducible results, even for temperature changes over time intervals that are much shorter than in scattering studies.

*The types of interactions control the temperature dependence of the thickness of the surface melt.* Heat capacities of argon and neon films adsorbed on uniform graphite substrates have shown strong increases at temperatures below the bulk transition, attributed to the progressive melting of the solid (Zhu and Dash 1986). Figure 2 shows the results for a series of films of different coverage. The increase is primarily due to the rate of conversion, i.e. to the temperature derivative of the melt layer thickness, varying as a power law, with an exponent approximately equal to  $-\frac{4}{3}$ , consistent with the dependence predicted for van der Waals solids.

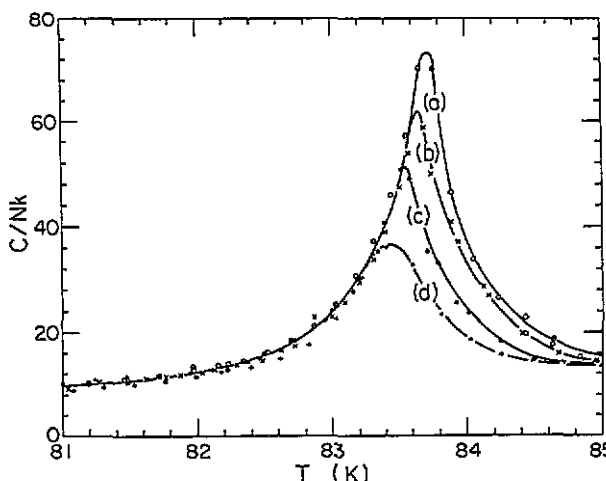


Figure 2. Heat capacity of argon films adsorbed on graphite, at temperatures near the bulk transition, showing precursors to the transition, with a common envelope and progression of the peak temperature with thickness (Zhu and Dash 1986). Thicknesses in atomic layers at 83 K are (a) 10.5, (b) 8.9, (c) 8.0, (d) 7.1.

In contrast, the temperature dependence of surface melting of Pb is logarithmic, as in equation (2.11). The exponential range dependence is attributed to screening of long-range

forces by conduction electrons. As the films thicken near  $T_0$  the temperature dependence tends to change to a power law (Pluis *et al* 1989, Trittbach *et al* 1994). The crossover is due to the more rapid weakening of the exponential attenuation, allowing the power law behaviour to shine through.

*Surface melting varies with the facet orientation.* The first experimental demonstration of anisotropy was produced by Stock and Menzel (1978) and Stock (1980), by thermal emission. The intensity of black-body radiation radiated from a hot metallic object to a colder environment depends on the electrical conductivity of the surface and, therefore, on its physical state. The radiation from a single crystal of copper was found to vary strongly with position on the surface; the brightness of some facets changed gradually as the melting temperature was approached, while others changed more abruptly. Stock and Menzel took the gradual changes to indicate the proportional development of a liquid layer on that particular facet, while adjacent facets remained solid up to the melting point. Pluis *et al* (1987) used ion backscattering to study surface melting anisotropy in Pb. The experiment was performed on a single crystal shaped into a cylindrical surface, so that different facets were exposed. As temperature approached  $T_0$  the backscattering intensity, indicating the degree of surface disorder, varied greatly with position. The (111) facet showed no increase beyond that due to thermal vibrations, but at increasing angles of inclination the backscattered intensity rose monotonically, indicating increasing thickness of surface melt. The results are shown in figure 3.

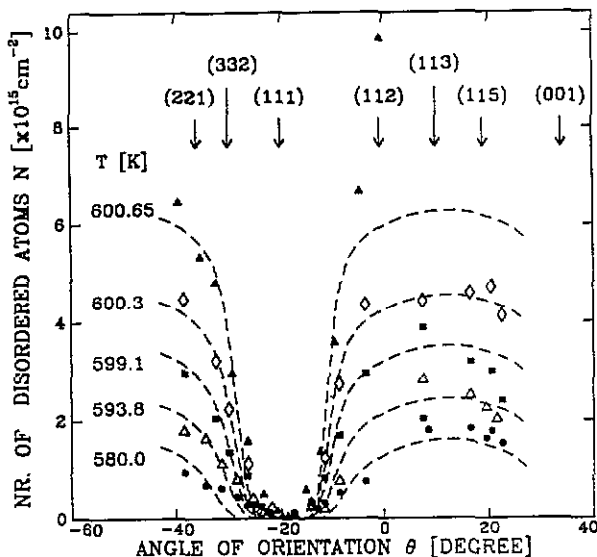


Figure 3. Thickness of the disordered layer on Pb crystal at various angles with respect to the [112] axis, in the neighbourhood of the bulk transition temperature (Pluis *et al* 1987).

Heyraud and Métois (1987) found that certain microscopic crystals of Pb superheated, i.e. remained solid a few degrees above the bulk transition. The crystal shapes indicated that their surfaces were composed completely of (111) planes, and the superheating was explained by Nozières (1989) as due to the absence of surface melting on those facets.

The anisotropy of surface melting depends on the range of the particle interactions. In contrast to the results on metals, the (111) planes of noble gas solids apparently do undergo surface melting. This was concluded by Maruyama (1989), from a study of equilibrium crystal shapes of small krypton and xenon crystals. The same conclusion is drawn from the surface melting of noble gas and molecular films adsorbed on graphite, because their structures are close packed and similar to (111) planes.

Several computer studies have explored the anisotropy. Valkealahti and Nieminen (1987) found that (111) planes of solids with truncated Lennard-Jones potentials undergo premelting. Häkinen and Manninen (1992) computed the structure and dynamics of a model of copper. They found that the order of stability with respect to melting follows the order of packing density: (110) disorders first; (111) remains ordered to the melting point. In agreement with experiments, premelting is lacking on (100). Carnevali *et al* (1987) studied reconstructed and unreconstructed Au (111) surfaces. They found no premelting on the reconstructed surface, but found that two atomic layers of the unreconstructed surface could melt well below  $T_0$ .

*Surface melting has a lower-dimensional analogue.* Abraham (1981) simulated two-dimensional systems of Lennard-Jones atoms, and found that a finite width band at the solid-vapour boundary broke down into liquid-like disorder at a temperature below the melting point of the solid. Figure 4 shows that the disorder is evidently an equilibrium phenomenon, in that the width of the disordered region did not increase as the number of computer steps was doubled, and doubled again. Experimental observations of *edge melting* were obtained a few years later by experiments with adsorbed films. Measurements on monolayers of neon (Zhu and Dash 1988, Pengra and Dash 1992), tetramethyl tin (Shechter *et al* 1990) and nitrogen monolayers (Chan 1990) showed the gradual premelting that is characteristic of surface melting in three-dimensional matter. Each of these systems have 'two-dimensional triple points', where monolayers adsorbed on basal plane graphite have vapour, liquid and solid phases coexisting in equilibrium with the bulk vapour.

*Thin liquid layers are more ordered in the proximity of solid walls.* The structure and dynamics of a liquid are changed in the neighbourhood of a solid wall, as a layer-like order is imposed by the boundary, a phenomenon sometimes called the *proximity effect*. All of its properties are modified, so that it becomes less fluid, and intermediate between those of the bulk solid and liquid phases. The ordering falls off approximately exponentially with distance, with a characteristic length typically equal to a few molecular diameters. The effect occurs at all solid boundaries, including the melting interface, where it blurs the boundary and causes the interface to have a finite width. Because of the rapid attenuation with distance, the ordering is unimportant except in very thin films, such as the quasi-liquid melt at temperatures somewhat remote from  $T_0$ . Theories of such 'smectic-like order' have been given by Evans (1979), Broughton *et al* (1981), Tarazona and Vicente (1985), Schick and Shih (1987), Curtin (1987), Chernov and Mikheev (1989) and Dietrich (1993). Figure 5 shows the computer results of Löwen (1994) for a Lennard-Jones system, showing both the increasing thickness of liquid on the approach to  $T_0$ , and its layer-like ordering near the crystal interface.

The ordering affects the dynamic and thermodynamic properties of very thin liquid films, e.g. causing an anisotropic decrease in mobility and a decrease in entropy. The latter has been observed in calorimetry of thin Ar and Ne films, as a lowered latent heat of fusion (Zhu and Dash 1986, 1988).

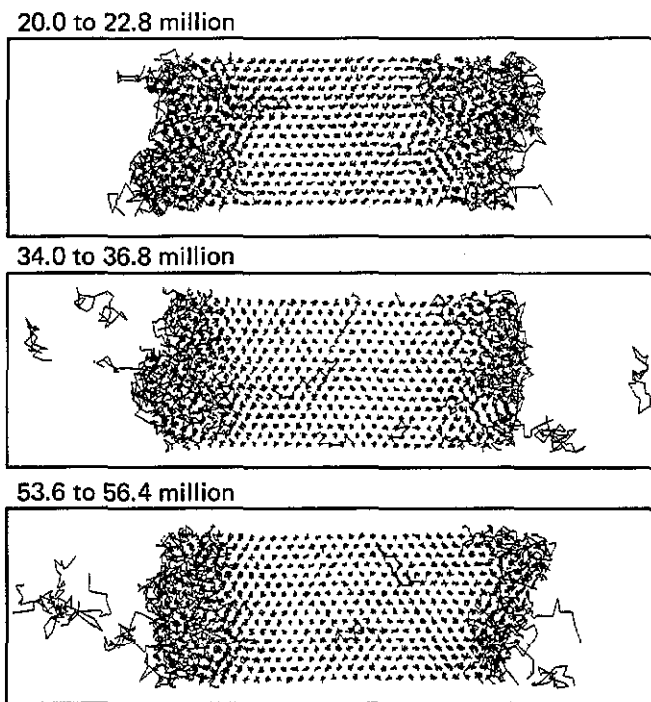


**Figure 4.** Monte Carlo computer simulation of the dynamics of a two-dimensional strip of solid argon just below its melting transition (Abraham 1981). The stable width of the disordered regions at the interfaces with two-dimensional vapour show that 'edge melting' is an equilibrium phenomenon.

*Surface disorder in surface melting is liquid-like.* Surface melting differs from other forms of surface disorder such as 'roughening'. In surface roughening the interface becomes densely covered with atomic steps and terraces, so that the location of the interface is indistinct. The change from the smooth to the roughened state is a second-order phase transition, which occurs at higher temperatures on facets with higher density. On close-packed surfaces of Lennard-Jones molecules the transition is near  $0.8T_0$ . Although the steps and terraces of the roughened surface are in dynamic equilibrium, the atomic motions are much slower and more highly coordinated than in liquids (Weeks 1979, den Nijs 1988). A characteristic and distinctive signature of surface melting, other than mobility, is the fact that it is pinned to the melting point of the bulk, in that the thickness of the melt is a function of the temperature difference ( $T_0 - T$ ) rather than of  $T$  alone. The indications of liquid-like mobility seen in computer simulations have been noted above. Quantitative experimental evidence has also been obtained using several different techniques. Binh and colleagues (1978, 1985) observed atomic migration on tungsten at high temperatures. At  $T/T_0 > 0.75$  the diffusion changed from a form indicating surface hopping to a more cooperative motion, as a kind of viscous flow. Quasi-elastic neutron scattering has been used to measure the diffusion in adsorbed hydrogen isotopes (Krim and Chiarello 1991, Gay *et al* 1992, Maruyama *et al* 1993) and in methane films. The diffusion constants are found to be of the same order of magnitude as that of the bulk liquid.

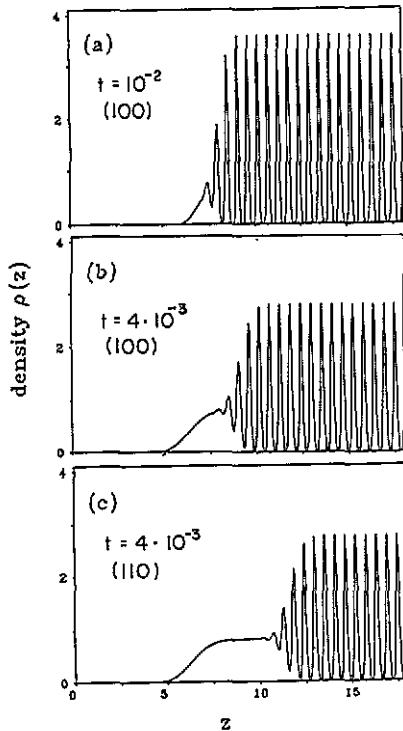


**Figure 5.** The density profile of liquid and solid in the proximity of the crystal–gas interface near the triple point, by an unconstrained variational calculation with Lennard-Jones atoms (Löwen 1994). The laterally integrated density shows the increased thickness of the melted layer as reduced temperature  $t \rightarrow 0$ , and the layer-like ordering of the liquid in proximity to the interface.

## 2.2. Interfacial and grain boundary melting

**2.2.1. Interfacial melting.** The focus here is on the interface between a solid and a non-reactive, uncorrugated substrate. We can readily translate the thermodynamic tenets of surface melting at the solid–vapour interface to this situation, by comparing the free energy cost of the wet system with that of the dry system at coexistence. The free energy associated with bringing the solid in contact with the wall is  $\gamma_{sw}$ . If the interface is wetted by the liquid phase, then this energy must be equivalent to that needed to create an intervening macroscopic layer of fluid. Hence, a necessary condition for *interfacial melting* is satisfaction of the equality

$$\gamma_{sw} = \gamma_{sl} + \gamma_{lw} \quad (2.12)$$

where the  $\gamma$ s are as previously, with implicit reference to the crystallographic orientations present at an interface.

**2.2.2. Grain boundaries.** Carrying over the treatment of the vapour and the wall, we examine the interface between two orientations of a solid; *twist* and *tilt* grain boundaries are the varieties generally discussed in the literature. But, although long-range interactions should suppress the formation of a disordered region of arbitrary macroscopic thickness, we

may expect to see some structural modification associated with the molecular reorientation. Grain boundary melting can nevertheless be defined when such an interface nucleates the liquid phase as  $T \rightarrow T_0$ . Intuition is gained from a simple picture in which we consider the boundary as being defined by a single angle  $\theta$  with interfacial energy  $\gamma_{ss}(\theta, T_0)$  (Broughton and Gilmer 1986). At  $T_0$ ,  $\gamma_{ss} \rightarrow 0$  as  $\theta \rightarrow 0$ , so that wetting is determined by whether or not the equality in

$$\gamma_{ss}(\theta, T_0) \leq 2\gamma_s \quad (2.13)$$

is satisfied at  $T_0$ . If the equality is satisfied, the boundary will be wet. The obvious importance of this problem for technological materials makes it an active field, and we do not attempt a thorough treatment here. Rather, we point out the guiding features of recent studies, and note that there are distinct structural variations at grain boundaries, but their features are system specific (Fionova and Artemyev 1993).

Two-dimensional lattice-gas models have predicted a high-density disordered phase at a grain boundary (Kikuchi and Cahn 1980). Well below  $T_0$  they found a gradual but clearly defined transition in (a) the thermodynamic properties and (b) the structure of the boundary. As  $T \rightarrow T_0$ : (a) the excess free energy remains finite and equals twice the solid-liquid interfacial free energy, while the excess entropy per unit length of the boundary diverges as  $-\ln(T_0 - T)$ . (b) the structure evolves continuously toward a liquid layer disjoining the misoriented crystals, the thickness of which has the above logarithmic divergence.

Anisotropy can exert a strong influence on the local interfacial disorder. This effect is exposed by studying the solid-melt interface in different symmetry planes. Using their earlier approach, Cahn and Kikuchi (1985) find a dependence on the crystal plane packing. In the non-close-packed case they find a smooth change from solid to liquid structure. In the close-packed case they find an intermediate region wherein long-range order in atomic planes parallel to the interface is lost, but an interplanar alternation in density occurs in the perpendicular direction. This alternate ordering disappears far from the interface. For FCC lattices, intermediate structure is found for the (001) boundary and smooth disorder for the (110) boundary. Similar liquid density oscillations have been found in cluster variational methods (An 1989), and in molecular dynamics calculations performed by Landman and his group (e.g. Xia *et al* 1992). Calculations of Lennard-Jones solids by Broughton and Gilmer (1986) have revealed similar qualitative behaviour with regard to the orientation dependence of grain boundary disorder and other interfaces (Broughton and Gilmer 1983a, b). Because of the continuous temperature dependence of the thermodynamic parameters, no true first-order transition for  $T < T_0$  can be associated with a particular state of interfacial disorder.

Evidence for grain boundary 'splitting' was found by Schick and Shih (1987) in their  $Z(N)$  model calculation of a twist mismatch grain boundary. The notion here is that at coexistence, the boundary is wetted not by a liquid, but by a solid of intermediate orientation. Of course, the implication is that this is a less costly configuration than wetting by a liquid. They point out that their result is consistent with some molecular dynamics simulations and that, for van der Waals materials, a calculation of the Hamaker constant using dispersion force theory (Dzyaloshinskii *et al* 1961) indicates incomplete wetting. The importance is that, although a given calculation may indicate that the dry grain boundary should decompose at coexistence, whether or not the new configuration is liquid or a solid of intermediate orientation may depend on the nature of the relaxation, and so on the details of the model†. An interesting recent study of the orientation dependence of the Hamaker

† Experimental evidence for the near complete wetting of grain boundaries by their melt has been found for FCC  $^4\text{He}$  (Franck *et al* 1983).

constant in non-cubic crystals appears to be ideal for addressing aspects of this issue (Dal Corso and Tosatti 1993).

### 2.3. Size effects in premelting

**2.3.1. Curved surfaces.** The interfacial energy between solid and melt liquid provides a mechanism whereby interface curvature can enhance or retard surface and interfacial melting, depending on the sign of the curvature (Baker and Dash 1989, Nenow and Trayanov 1990, Kofman *et al* 1993). Enhancement occurs if the interface is concave as viewed from the solid side. For relatively large radius of curvature,  $r \gg d$ , the increased thickness  $d'(T)$  on a spherical surface is (Baker and Dash 1989)

$$d'(T, r) = d(T) \left( 1 + \frac{2\gamma T_0}{3\rho_s q_{sl} r} (T_0 - T) \right). \quad (2.14)$$

Equation (2.14) predicts that the surface melt on a particle in vapour is thicker if the solid radius is smaller. Therefore, as  $T$  rises melting increases, until the radius of the solid shrinks to a critical value, where melting is completed abruptly. A related effect, discussed below, has been known for many years.

**2.3.2. Solid particles immersed in melt liquid.** The equilibrium temperature of small solid particles in the melt liquid is lower than that of large solid samples, due to a combination of surface energy and interface curvature (Thomson 1871, Gibbs 1906), now known as the Gibbs–Thomson effect. Consider an isotropic solid object of area  $A$  in equilibrium with its melt liquid. The free energy of the system is the sum of the bulk phase and interfacial contributions:

$$G = G_s + G_l + G_{int} = N_s \mu_s + N_l \mu_l + A \gamma_{sl} \quad (2.15)$$

where  $\mu$  is the chemical potential and  $\gamma_{sl}$  is the free energy coefficient of the solid–liquid interface. At equilibrium,  $G$  is a minimum with respect to mass exchange between the phases. This condition, together with mass conservation, yields

$$\Delta\mu \equiv (\mu_s - \mu_l) + \gamma_{sl} (dA/dN_s) = 0. \quad (2.16)$$

The surface term shifts the location of equilibrium. The new pressure and temperature coordinates are found by an expansion, as in section 2.1.

The derivative  $(dA/dN_s)$  in equation (2.16) can be expressed in terms of the surface curvature. For a point on the surface with two principal radii of curvature, the shift is

$$\Delta T_0 = (1/r_1 + 1/r_2) \gamma_{sl} T_0 / \rho_s q_m \quad (2.17)$$

where  $\Delta T_0 \equiv T_0 - T$ , and  $r$  is measured as positive if the interface is concave toward the solid. For a sphere of radius  $r$ ,  $(dA/dN_s) = 2/\rho_s r$ , and this leads to an expression for the melting point shift

$$\Delta T_0 = 2\gamma_{sl} T_0 / \rho_s q_m r. \quad (2.18)$$

But the new equilibrium point is *metastable*. Consider a small particle slightly larger than the equilibrium value; to move toward equilibrium, the particle must melt slightly. This requires it to absorb heat from the remaining solid and the surroundings, which

causes local cooling, thus driving the system further from equilibrium. The converse, a particle slightly smaller than the equilibrium value, is likewise unstable, hence the liquid at equilibrium is completely clear of solid particles. But a stable temperature shift exists when the solid–liquid interface curvature is reversed, as in pores and crevices where liquid wets the solid–wall interface. In this case melting leads to an increase of the radius of curvature of the solid–liquid interface, so that fluctuations from equilibrium are damped, and a definite curvature-induced shift is produced. As discussed in section 5, this effect is important in frozen soils.

**2.3.3. Melting of particles in vapour.** The shift equations (2.17) and (2.18) cannot apply to a ‘dry’ powder in vapour unless the particles are already covered by the melt liquid. If liquid does not wet the solid at  $T_0$ , the melting temperature is *raised above* the melting point; i.e. the liquid phase must be *nucleated*. The size dependence has been observed in experiments with gold particles in vapour (Buffat and Borel 1976), and since there was no nucleation threshold it was concluded that the surfaces were coated with liquid below the melting point. Since, with rare exception, melting is not a nucleated process (Ubbelohde 1965), it can be concluded that melt liquid typically wets the solid at  $T < T_0$ ; that surface melting exists on one or more of the principal facets of interfaces with vapour for virtually all materials. Important exceptions have recently been observed in certain very small Pb crystals, and are discussed earlier (see section 2.1.2 and figure 3).

#### 2.4. Surface disorder

**2.4.1. Rough substrates.** Disorder at a solid–wall boundary will tend to induce premelting, by raising the interfacial energy of the solid relative to the liquid, through strains, defects, polycrystallinity or multifaceting. There are several forms of disorder in the wall that can produce such effects: roughness, polycrystallinity, dislocations and impurities; essentially all of the forms of disorder that can cause heterogeneous adsorption. Roughness increases the contact area to both liquid and solid and in this regard does not discriminate between them. However, roughness forces the solid to present unfavourable high-energy facets for solid–wall contact, while the liquid is compliant because of its isotropy. We note several types of conditions which involve these effects.

The interfacial energies of solid He at walls of pressure cells (Balibar *et al* 1979, Landau *et al* 1980) have been found to be surprisingly high. In copper and glass chambers the solid He–wall interfacial tension  $\gamma_{sw}$  is greater than the liquid–wall tension  $\gamma_{lw}$ , leading to solid He–wall contact angles  $\theta > 90^\circ$ . The result is surprising because the attraction to the wall is expected to cause the solid to wet the wall, because of its higher density. In agreement with this expectation, experiments with  $^4\text{He}$  and  $^3\text{He}$  on well-ordered graphite and MgO surfaces (Landau and Saam 1977, Wiechert *et al* 1982) show preferential formation of solid and prefreezing. An explanation is given (Dash 1982) in terms of surface disorder, that a high density of nucleation sites on the disordered substrate produced a fine polycrystalline structure in the adjacent solid He, with a correspondingly large grain boundary energy. While it is possible that the initial state of the solid could be polycrystalline immediately after rapid freezing, the solid will tend to anneal, forming a small number of large crystals. The total area of contact between a large crystal and the substrate may not cause more than a small increase in the chemical potential. On the other hand, the irregularities and roughness of the substrate will force the contacting crystal to terminate in a range of surface orientations, with corresponding variations in the interfacial energy. Since the surface energy of a crystalline solid  $\gamma_{sw}(\phi)$  varies sharply around the orientation of the principal facets, as seen in a typical Wulff diagram (Wortis 1988), relatively mild roughness of a substrate

may produce appreciable increases in the average coefficient, and modify film growth (Dash 1990).

**2.4.2. Premelting in porous media.** The confinement of a material within a porous medium can result in an important reduction of the material's melting temperature. Many studies have been made of the effect in ice, particularly in soils, but we reserve their discussion for later. Here it is instructive to review observations of simpler molecular solids in porous glass and zeolites:  $^4\text{He}$  (Brewer *et al* 1978, Beamish *et al* 1983, Liezha *et al* 1986, Shimoda *et al* 1986, Kondo *et al* 1987, Hiroi *et al* 1989),  $\text{H}_2$  and  $\text{D}_2$  (Tell and Maris 1983, Amaya *et al* 1987, Brewer *et al* 1990, Rall *et al* 1991), Ne (Tell and Maris 1983) and Ar (Molz and Beamish 1992). In all of these systems melting begins appreciably below the bulk transitions when the pores are filled, although the first one or two adsorbed layers of the same substances *prefreeze*. Still another contrast is that  $^4\text{He}$  does not premelt in laminar graphite foils, whether adsorbed as a film, or condensed to fill the spaces (Landau and Saam 1977).

These apparently conflicting results are due to a competition between adsorption, confinement and disorder. The *prefreezing* of the first few adsorbed layers is due to strong substrate forces, as discussed in the previous section. The thickness of solid film is limited, so that beyond the critical thickness additional deposits form bulk crystallites on top of the disordered film. In contrast, full pores leave no possibility of partial wetting, for there is no room to reduce the area of contact with the disordered film. At moderate distances from the substrate the solid tends to be ordered, even if it was initially polycrystalline immediately after filling and cooling to low temperature. Depending on the temperature, the crystallites will tend to grow and merge into one or a small number of distinct crystals, due to the tendency to reduce the grain boundary energy. In the limiting case, each pore will be filled with a single crystal inside a cavity lined with a dense, disordered film of the same substance, which acts as a thermodynamically distinct, inert wall. In contrast to the equilibrium shape of a free crystal, the surface of the solid confined in a pore must have all possible orientations, so that the interfacial energy between the crystal and the wall will vary around the surface. The equilibrium orientation of the crystal will minimize the interfacial energy, which is a convolution of the polar angle dependence of the surface coefficient of the solid–wall boundary  $\gamma_{sw}(\phi)$  with the geometry of the pore. The regions where the interfacial coefficient  $\gamma_{sw}$  is particularly high will have especially large negative values of the wetting coefficient  $\Delta\gamma$ , where premelting begins when the crystal is warmed. (In cases where the core is composed of a small number of crystals, premelting may occur in the grain boundaries as well as at the wall interface.) As the temperature rises the melting spreads to other orientations, and the solid tends toward a more compact shape. If the solid–liquid interfaces are thermodynamically rough, the contours of the solid are rounded. In the limit the remaining solid becomes a sphere, which melts abruptly at a temperature below the bulk transition. The shift of the melting point is approximately equal to the  $\Delta T_0$  of equation (2.18). A minor difference is due to the finite thickness of the premelted liquid, which injects a certain dependence on pore geometry.

## 2.5. Supercooling, stability and nucleation

Two and three dimensionality blend at surfaces, and the issue of phase stability distinguishes the behaviour of premelted and bulk liquid. A *bulk* crystal is constructed by replication of unit cells. However, *bulk* liquids (or glasses) possess no such long-range order in the molecular configuration. The absence of long-range order under liquefaction actually provides stability due to the substantial gain in entropy. When  $T < T_0$ , the bulk liquid

is *supercooled* and *metastable* in the sense described in section 2.3.2. Hence, there is an appreciable probability that the solid phase will be nucleated. Unlike the bulk, a premelted film is *stable* at  $T < T_0$ . Here we briefly review nucleation theory in order to clearly present the distinction between bulk and interfacial transitions. The theory is well developed, dating back to Gibbs, and we simplify both general treatments (Turnbull 1956, Feder *et al* 1966) and those for ice (Fletcher 1970, Hobbs 1974).

For bulk volumes of most materials the degree of supercooling increases with a decrease in the concentration of insoluble foreign particles. Supercooling is also aided if the material is in the form of small droplets, which confine the particles to a smaller fraction of the total volume. The implication is that the freezing transition is enhanced by the presence of foreign particles. Intuition is gained by considering the nucleation process in the absence of such particles: *homogeneous* nucleation.

The freezing of a supercooled fluid of high purity is driven by the thermally activated formation of a small crystallite which grows at the expense of the liquid. Small crystallites are energetically costly due to the large surface-to-volume ratio which has a positive interfacial free energy contribution. Considering the crystallite containing enough molecules to be treated as a continuum, and that the anisotropy of the interfacial coefficients can be ignored, as in equation (2.15), we write the total free energy of formation of a cluster of radius  $r$  as

$$\Delta G = N_s(\mu_s - \mu_l)c_1 r^3 + c_2 \gamma_{sl} r^2 \quad (2.19)$$

where the  $c_s$  are geometrical constants and  $N_s$  is the number of solid molecules in the cluster. The above statement is now clearly displayed. In a supercooled liquid  $\mu_s < \mu_l$ , and the bulk term lowers the free energy, but for very small clusters the interfacial term dominates and the free energy increases with cluster radius.  $\Delta G$  reaches a maximum at a critical radius,  $r^*$ , and then all clusters of radius greater than  $r^*$  decrease  $\Delta G$ , and so grow thereby. Hence, the freezing process in a pure bulk fluid requires the climbing of an activation barrier  $\Delta G(r^*)$ , and supercooled liquid is metastable.

In equilibrium, if detailed molecular kinetics are ignored, the number of solid clusters per volume with radii  $r^*$  that will form in the liquid of  $n_l$  molecules per volume can be written

$$n_s = n_l \exp[-\Delta G(r^*)/kT]. \quad (2.20)$$

In metals, the nucleation frequency increases by an order of magnitude per degree of undercooling (Turnbull 1952, 1956). But, although there is a high probability of nucleation in supercooled water, substantial supercooling (more than 30 °C) can be obtained at atmospheric pressures (Franks 1982). A common explanation for this observation concerns the high concentration of non-ice-like hydrogen-bonded structures that occur naturally in water, so that ice-like clusters may account for only a small fraction of the bulk.

The addition of a foreign particle to the bulk liquid may lower the activation energy by acting as a substrate to nucleate a crystallite: *heterogeneous* nucleation. The ubiquity of such particles in the environment is evidenced by the minimal supercooling observed in many geophysical situations, and the details of heterogeneous nucleation have profound consequences for practical problems such as cloud seeding (e.g. Hobbs 1974, Fletcher 1970). In the latter area, the historical focus has been on particles with ice-like structure. In the context of interfacial melting (2.2) an ideal 'ice nucleus' would be one that suppresses interfacial premelting. Hence, the nucleus is treated as the wall in section 2.2, and the free energetic cost of forming a solid layer on a nucleus of area  $A_{sw}$  is

$$\Delta G = \Delta G_b + \gamma_{sl} A_{sl} - (\gamma_{wl} - \gamma_{sw}) A_{sw} \quad (2.21)$$

where  $\Delta G_b$  is the bulk contribution of the solid layer and the remainder are the interfacial terms. Naively treating the premelting condition for a 'planar' nucleus, water does wet the nucleus–ice interface when  $\Gamma = (\gamma_{wl} - \gamma_{sw})/\gamma_{sl} = -1$ , and does not wet the nucleus–ice interface when  $\Gamma = 1$ . In the former case the interfacial contribution to  $\Delta G$  is  $\gamma_{sl}(A_{sl} + A_{sw})$ , and in the latter case it is  $\gamma_{sl}(A_{sl} - A_{sw})$ . Hence, the activation barrier to heterogeneous nucleation can be expressed in terms of the interfacial coefficient  $\Gamma$  and the dimensions of the nucleus. As  $\Gamma$  neglects orientational and steric effects, among others, this is only a heuristic treatment but conveys the overall qualitative effects. Fletcher presents the critical undercooling as a function of nucleus size and  $\Gamma$  for supercooled water. This shows that for a nucleus with  $\Gamma = -1$  and radius of  $10\text{ }\mu\text{m}$ , water must be supercooled by more than  $35\text{ }^\circ\text{C}$  to activate ice formation.

The contrast between supercooled bulk liquid and premelted films can be understood conceptually as follows. Introducing a solid particle of supercritical dimensions  $r > r^*$  into the bulk liquid initiates solidification, yet the thin premelted film remains liquid in direct contact with the solid phase. Hence, at the same temperature, the bulk requires the absence of solid to maintain liquidity and the interfacial film would *not be present* in the absence of the solid interface. At interfaces, the cost of maintaining a liquid-like structure is paid for by the benefit of lowering the surface free energy of the *system*. In the bulk liquid, the surface energy assesses the penalty, as there is only one choice of interfacial coefficients (in homogeneous nucleation), and the bulk free energy drives the conversion. (A convincing and simple exercise is to compare the implications of equations (2.18) and (2.9).) One might think of the ability of water to be deeply supercooled as being intimately related to its *inability* to nucleate the solid from the free surface (Elbaum and Schick 1991b). Thus, understanding the asymmetry between superheating a crystal and supercooling a bulk liquid lies in interfacial phenomena. As seen above, the case of heterogeneous nucleation exhibits both the bulk and interfacial concepts.

Molecular fluids such as water defy simple structural descriptions, whereas monatomic fluids are disordered aggregations of atoms with no orientational preference in a unit volume greater than the coordination number. Yet the non-universality of a nucleation barrier is tied to the details of the intermolecular forces, and even in atomic liquids a complete theory has been elusive (Oxtoby 1990). General studies approach the transition from the liquid side, using density functional theory and computer simulations. In the former, a solid is thought of as an inhomogeneous liquid with a density that is functionally related to a structure factor. The structure factor can be determined experimentally or can be calculated using an assumed potential (e.g. noble gases are well captured with a Lennard-Jones pair potential). Computer studies utilize a number of potentials and in some cases compare favourably with density functional theory (Oxtoby 1990).

The theories of water structure attempt to create an instantaneous picture of the molecular configuration. A thorough qualitative discussion of early work can be found in Fletcher (1970). The extensive degree of hydrogen bonding in water, and its tetrahedral structure, give rise to a great deal of local variation associated with the bending, stretching and continuous creation and destruction of bonds. When the spectrum of these distortions is continuous and each molecule experiences the same environment, a homogeneous picture emerges. Yet computer simulations (e.g. Blumberg *et al* 1984) have supported the picture of water as a mixture of two or more structures each having a specific bonding configuration. Here, there is a continuous creation and destruction of heterophase clusters (on ps timescales) associated with regions of high bond connectivity. There is some agreement on consistency among potentials (Karim *et al* 1990), but much recent effort has focused on distinguishing between the existence of a spinodal point or a critical point in the phase behaviour

of supercooled water at pressures near  $10^3$  atm (e.g. Poole *et al* 1993a, b). With the possible exception of interfacial phenomena related to the polymorphs of ice (Whalley *et al* 1991), this critical behaviour is unrelated to our particular focus. Recent x-ray scattering measurements of H<sub>2</sub>O structure factors in the range  $-34 < T < 25$  °C provide estimates of water correlation lengths and isothermal compressibilities (Xie *et al* 1993). They found no change in the correlation length with supercooling, indicating that increasing density fluctuations are associated with an increase in the cluster size rather than an increasing correlation length.

Given the daunting task of understanding the bulk solid–liquid transition in general, and the added complications associated with water structure, it is not surprising that a microscopic or semi-microscopic picture of premelted water does not exist. Indeed, bulk supercooled water needs to be understood at this level before adequate intercomparison with water films can be made. The wetting properties of liquids in pores and capillaries are being extracted using some of the same theoretical procedures as discussed above (Evans 1990, Schick 1990, Israelachvili 1992), so the future is promising. Under well-controlled equilibrium conditions the features of surface phases have been extensively studied in a variety of materials (Dash 1975). However, what dominates many of the environmental effects of ice interfaces concerns the *approach* to a stable, supercooled, equilibrium state, and the effects of impurities.

### 2.6. Solutes: solid–liquid distribution

In the laboratory, great effort is expended in order to obtain purity in a given sample, whereas in nearly every geophysical setting, phase coexistence will be altered by the presence of impurities. Typically, the impurity concentration is dilute, and the solution can be treated as *ideal*. By this it is meant that the concentration of solute molecules is low enough that they do not interact; the solute simply dilutes the solvent. At constant pressure, impurities shift the equilibrium temperature by an amount which depends on the solute concentration. For a solution consisting of  $n_j$  moles of solute in  $n$  moles of solvent, Raoult's law expresses this shift as

$$T_c = T_0 \left( 1 - \frac{RT_0}{q_m} \frac{n_j}{n} \right) \quad (2.22)$$

where  $R$  is the gas constant and  $q_m$  is the heat of fusion of the solvent. In practice,  $T_c$  is related to the solute concentration in the liquid  $C_l$  by an empirical liquidus slope  $m$ ;  $T_c = mC_l$ . The ideal slope given by equation (2.22) is  $m = -103.07$  K with  $C_l$  expressed as a molar ratio, but empirical slopes are generally applied in the concentration range of particular interest to a given problem. For example, for NaCl solutions with  $C_l \approx 0.011$  the empirical slope is  $m \approx -178.04$  K. More detailed values have been tabulated by electrolyte chemists (Partanen and Lindström 1991).

Impurities adsorbed at interfaces reduce the associated free energy in a manner analogous to bulk energies. Because the impurities are non-volatile and insoluble in ice, the interfacial coefficients in  $\Delta\gamma$  will be reduced, but because of the low density of the vapour,  $\gamma_{sv}$  may be reduced to a lesser extent. Hence, surface melting may be enhanced relative to the pure case. Experimentally, impurities may have modified surfaces of ice against air (Elbaum *et al* 1993), although the impurity species was unknown. A related effect concerns the wetting of an ionizable substrate by water. De Gennes (1985) has pointed out that when the Debye screening length  $\kappa_d^{-1}$  is much larger than the width of the liquid–vapour interface, the long-range repulsive behaviour is modified and can cause a shift in both the order of the transition

and the associated temperature. The impurity-induced variation of ion concentration may lead to qualitatively similar effects in interfacial melting.

In equilibrium, the solute concentration of a given species in ice is much less than that in solution, and this is commonly represented by the *equilibrium distribution coefficient* for that species:

$$k_e = C_s/C_1 \quad (2.23)$$

where  $C_s$  is the equilibrium concentration in the solid. In a subeutectic solution  $k_e < 1$ , and decreases with the degree of lattice mismatch. In most aqueous solutions studied  $10^{-4} < k_e < 10^{-1}$  (e.g. Gross *et al* 1987), so that ice grown slowly from solution remains nearly pure. This idealization is of great advantage in extracting the essential features of a system even though one is often actually dealing with a multicomponent system which is dominated by a particular impurity species. At this level the solid–liquid impurity distribution is conceptually tractable, yet even in water of high purity, there are finite concentrations of thermally activated intrinsic ions  $\text{H}_3\text{O}^+$  and  $\text{OH}^-$ , which are phase dependent. The complications grow rapidly on consideration of the kinetics of a solution and when crystallization occurs. Due to the environmental relevance, we touch on the issues of relevance to solidification.

In most aqueous solutions the solute dissociates, and preferential interfacial ion adsorption and solid–liquid segregation can lead to a plethora of processes, not all of which are independent. Hence, one may have ionic distribution coefficients,  $k_e^+$  and  $k_e^-$ . Yet, these and related effects are observed to vary immensely with concentration of a given solute, pH, and between various chemical species. This is mainly due to species-specific kinetics and the number and magnitude of experimental difficulties which can mask essential behaviour. Gross *et al* (1977, 1987) have examined these difficulties, but many still remain. The crucial issues are as follows. (a) Since the density of the solution depends on both temperature and solute concentration (typically an order of magnitude more sensitive to changes in the latter), samples may be modified by convection. (b) During growth there is a possibility of phase boundary instabilities (see section 5.3.2) which can result in the trapping of impurities in bulk. (c) Some species show a clear concentration dependence of  $k_e$  and others do not. (d) Measurements near the solubility limit or the eutectic points are difficult to interpret. Finally, in almost all cases above some threshold growth rate, there will be a growth rate dependence to the distribution (e.g. Aziz 1982), implying the measurement of an *effective* distribution coefficient  $k_{\text{eff}}$  rather than an equilibrium quantity. Since many of the above effects couple, it is common to measure the bulk concentrations before and after an experiment, and express the net effect in terms of  $k_{\text{eff}}$ . We note that Tiller (1991) has introduced two additional distribution coefficients in order to delineate a number of basic issues: an ‘interface coefficient’ that describes interfacial adsorption of impurities, and a ‘net coefficient’ that describes the dynamical modification of the interfacial region.

Since preferential ion incorporation may lead to an effect which is possibly of relevance to environmental problems we discuss it here, in its basic context of solute distribution. The observed formation of an interfacial electric field during growth of ice from dilute solutions has been associated with Workman and Reynolds (e.g. Hobbs 1974). An example for a monovalent ionic solution might be an electrical imbalance associated with the preferential  $\text{Na}^+$  rejection during the growth of ice from a dilute aqueous  $\text{NaCl}$  solution. A recent theory (Bronshteyn and Chernov 1991) would posit the trapping of a line of negative charge density parallel to a newly formed *planar* freezing front. This induces an electric

field between the solid and the rejected liquid cations, thereby creating a Debye double layer on the liquid side of the interface. Of course, the screening length will be a dynamical quantity due to the moving crystallization front. Charge redistribution is obtained from a number of well-known processes: in the solid it is accommodated by the mobility of Bjerrum and ionization defects, and in the liquid it is determined by the dissociation rates and diffusion coefficients. Rates of neutralization are strongly phase dependent due to the higher concentration of intrinsic ions in the liquid and the disparity in the solid and liquid mobilities. Bronshteyn and Chernov (1991) predict that a freezing potential only arises when the product of the impurity concentration at the interface and the mean growth rate exceed a critical value that depends on the acidity. The comparison of the theory to experiment is limited by the indetermination of the stability of the solidification front. Chernov (1993b) has recently reviewed growth from aqueous solutions.

Finally, we note that  $k_e$  will depend on crystallographic orientation. This will be especially relevant in growth from a seed which contains both facets and rough orientations, presenting the impurity with attachment sites whose energy varies with orientation. In the pure case, especially in ice, such growth is highly anisotropic (Elbaum and Wetlaufer 1993, Furukawa 1993, Wetlaufer 1994), and we expect anisotropy in solute distribution as well. Some time ago, thorough studies supporting orientation dependence were performed on semiconductors (e.g. Tiller 1991), yet little effort has gone into examining this question for ice.

### 3. Premelting of ice. Laboratory studies

Surface melting and interfacial melting are fundamentally the same phenomenon, but they demand quite different experimental techniques. In addition, their wetting coefficients  $\Delta\gamma$  are distinct and experimental uncertainties, impurities and disorder effects are peculiar to each, so that results from one do not necessarily carry any implications for the other. For these reasons they are treated separately in this review.

#### 3.1. Vapour interfaces

The surface melting of ice at interfaces with vapour and gaseous atmospheres has been studied in several laboratory experiments, with extremely variable and complex results. The variability may be due in part to great sensitivity to the atmosphere and conditions of preparation, but also to inherent differences in measurement technique. While several studies have shown liquid-like surface films at temperatures well below the bulk transition, others have seemed to prove that ice does not surface melt. The evidence of surface melting comes from studies by proton backscattering (Golecki and Jaccard 1978), ellipsometry (Beaglehole and Nason 1980, Furukawa *et al* 1987) and x-ray diffraction (Furukawa *et al* 1988, Lied *et al* 1994). Golecki and Jaccard (1978) observed a disordered surface layer on ice in pure vapour above  $-50^\circ\text{C}$ , increasing in thickness with temperature to more than 800 Å at  $-2^\circ\text{C}$ . Beaglehole and Nason (1980) reported a liquid-like layer on the prism face in air above  $-20^\circ\text{C}$ , increasing in thickness to 130 Å at  $-1.5^\circ\text{C}$ . Furukawa *et al* (1987) found liquid-like layers on the prism face above  $-4^\circ\text{C}$  and on the basal face above  $-2^\circ\text{C}$ , both thickening rapidly with further warming. Kouchi *et al* observed diffuse scattering, presumed to be due to liquid-like films, equally strong on surfaces of polycrystals and prism and basal facets of a single crystal, at temperatures at least as low as  $-2.1^\circ\text{C}$ . Lied *et al* (1994) observed quasiliquid on the same facets, but at much lower temperatures.

In contrast, two studies of crystal growth have led to the conclusion that ice does not surface melt completely. Direct visual observation of standing droplets of water at temperatures just below the triple point indicate that water does not wet (*i.e.* *completely wet*) ice-vapour interfaces (Ketcham and Hobbs 1969, Knight 1971). Contact angles were extremely small but nevertheless finite, and it was concluded therefore that ice does not surface melt.

A resolution to this controversy has come recently, through experimental and theoretical studies. The experiment was carried out by optical reflectometry and interference microscopy (Elbaum *et al* 1993). The surfaces of prism and basal facets were examined, in pure water vapour and in air, at temperatures from below  $-10^{\circ}\text{C}$  to the melting point. Prism facets showed no surface melting in pure vapour or air, up to a roughening transition at  $-1.35^{\circ}\text{C}$ . Basal facets in pure vapour showed surface melting beginning at or slightly below  $-2^{\circ}\text{C}$ . However, since the experiment could not resolve film thicknesses less than 12 Å, surface melting could have begun at much lower temperature. Above  $-2^{\circ}\text{C}$  thickness increased with  $T$  up to a few hundredths of a degree below bulk melting, when droplets suddenly appeared on the surface. The droplets were stable and reproducible on temperature cycling. This was a novelty, indicating the *incomplete wetting* of the quasi-liquid film by the bulk liquid. The results were explained by Elbaum and Schick (1991a) with a detailed calculation based on the theory of wetting under polarization forces (Dzyaloshinskii *et al* 1961). In general, wetting occurs when the polarizability of the substrate is greater than that of the film. In the case of water films on ice, the polarizabilities at high frequency favour wetting; at low frequencies non-wetting is preferred. For thin films, the whole range of frequencies is important; the high-frequency contributions outweigh those of low frequencies, and the net result is wetting. But at longer range the high-frequency interactions become attenuated by time delays between the film and the substrate, an effect known as 'retardation'. Then cohesion wins out, the adhesion to the ice fails at some limiting thickness, and wetting is incomplete. The temperature dependence of the film thickness, calculated by Elbaum and Schick, is shown in figure 6.

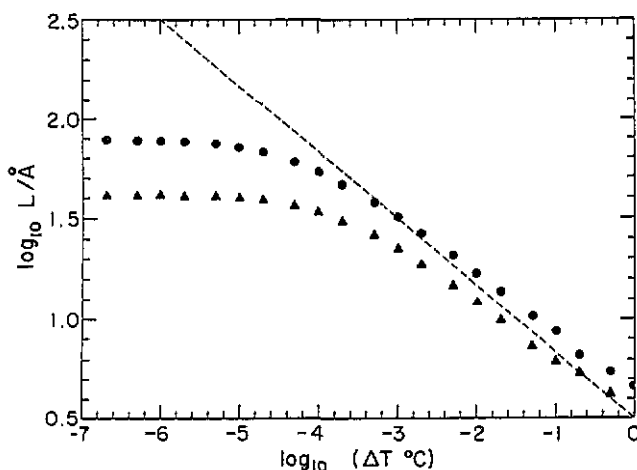


Figure 6. The thickness of the surface melted film on ice as a function of the temperature below the triple point, calculated by Elbaum and Schick (1991a). The broken line shows the result without retardation, and the solid line with retardation. The circles and triangles correspond to different sets of data on polarizabilities.

The phenomenon of *incomplete surface melting* explains the apparent conflict between the observations of surface films by ellipsometry and the non-wetting droplets seen by microscopy; unexpectedly, the two effects coexist. New calculations of ice against various substrates reveal examples of both complete and incomplete interfacial melting, and non-melting (Bar-Ziv and Safran 1993, Wilen *et al* 1994). Recent studies have shown yet another system exhibiting incomplete surface melting: Ge (111) facets (Takeuchi *et al* 1994). The remaining discrepancies among the various measurements may be due to the sensitivity of the films to surface disorder and impurities. There is evidence of surface melting in atmospheres containing soluble gases, at lower temperatures than in pure vapour (see section 5.3). Such an effect, termed *impurity-stimulated surface melting*, has been discussed by Beaglehole (1991).

### 3.2. Interfacial melting at solid walls

The persistence of unfrozen water in subzero soils, to temperatures as low as  $-40^{\circ}\text{C}$ , has been known to soil scientists and geologists for many years (Anderson and Morgenstern 1973), but there has been no agreement on the cause of the premelting or the nature of the unfrozen water. The controversy has been sustained by the complexity of typical soils and the variety of their chemical and electrical interactions. However, many of the uncertainties have been removed or sharply reduced in a number of recent experiments with more completely characterized substrates and geometries: quartz (Barer *et al* 1977, Fu 1993), metals and alloys (Gilpin 1980a), graphite (Maruyama *et al* 1992, Gay *et al* 1992), talc (Maruyama *et al* 1992), glass (Furukawa 1993, Beaglehole and Wilson 1994), silica (Bellissent-Funel 1993, Fu 1993) and polystyrene (Fu 1993).

Among the most detailed results are those obtained in an earlier study, 'Wire regelation', in which a weighted wire slowly sinks through a block of ice (Gilpin 1980a). A common interpretation of wire regelation is that local melting occurs under the wire due to the local pressure, and refreezing occurs above, the rate being controlled by heat conduction across the wire. While pressure melting is the dominant mechanism if the temperature is sufficiently close to  $0^{\circ}\text{C}$ , the temperature range in the main part of Gilpin's study was too low for this effect. Nevertheless, the motion continued, at temperatures as low as  $-35^{\circ}\text{C}$ . The motion was analysed in terms of the viscous resistance of a layer of unfrozen water around the wire. Assuming that the viscosity of the layer was equal to that of supercooled bulk water of the same temperature, the results yielded a layer thickness varying as a power law in the temperature, with empirical exponent  $-0.42$  down to  $-10^{\circ}\text{C}$ . A reexamination of Gilpin's data found that the data are consistent with the theoretical van der Waals exponent  $-\frac{1}{3}$  in a more limited temperature range, where the calculated thickness is at least  $20\text{ \AA}$  (Dash 1989a). At lower temperature the data indicates higher effective viscosity, consistent with the expected proximity effect in a very thin film (see figure 7).

The possible role of substrate chemical interactions and the microscopic nature of the premelted film, whether liquid like or static disorder, were examined by quasi-elastic neutron scattering (QENS), which allows the simultaneous measurement of the unfrozen fraction and its mobility (Maruyama *et al* 1992). The study was performed with  $\text{H}_2\text{O}$ -saturated powders of graphitized carbon black and talc. Graphite was chosen because of its inertness, to test whether premelting of ice is necessarily due to chemical interactions or electric double-layer effects involving the water molecules and the substrate. The positive results on graphite in this and a later study (Gay *et al* 1992) and a subsequent study of polystyrene (Fu 1993) indicated no evident dependence on the chemical nature of the substrate. The QENS results showed that the diffusion coefficient of the quasi-liquid layer is approximately equal to that of supercooled water.

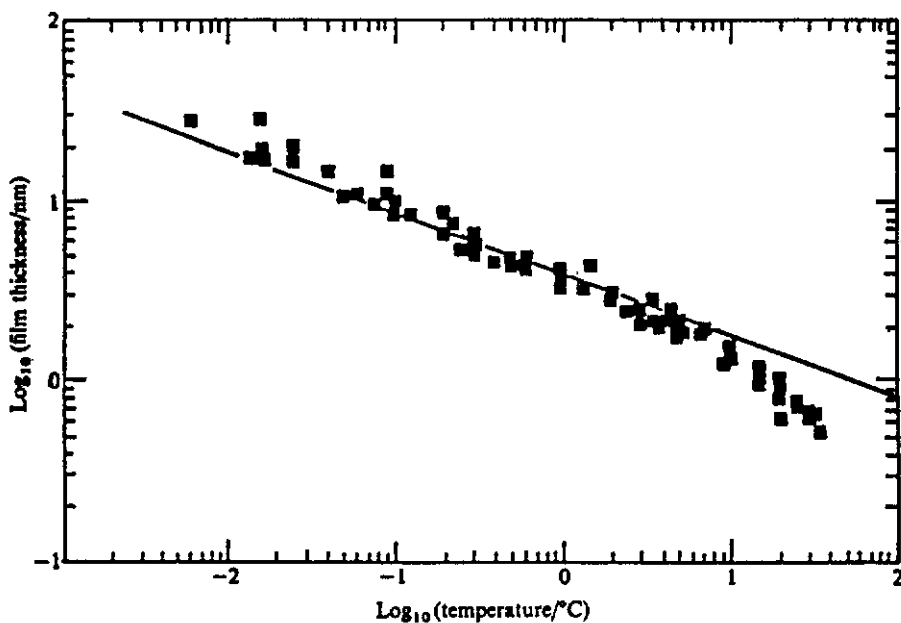


**Figure 7.** The thickness of the water layer around wires imbedded in ice, from a study of wire regelation (Gilpin 1980a). The line is a power law with exponent  $\frac{1}{3}$ , corresponding to the theoretical dependence for surface melting which may be controlled by dispersion forces (Dash 1989a). The discrepancy at low temperatures may be due to the proximity effect and the coefficient in the power law may be explained by other interactions (Wilen *et al* 1994).

The role of surface curvature was examined in studies with monosized artificial powders of spherical particles (Maruyama *et al* 1992, Cahn *et al* 1992). Cahn *et al* analysed premelting in close packed powders of spherical particles as a composite of surface melting at particle interfaces and grain boundaries, and curvature-depressed melting point at crevices and grain boundary junctions. Their calculations, involving no adjustable parameters, are in good agreement with measurements in graphitized carbon black and polyethylene spheres (figure 8). The same principles were applied to the analysis of neutron diffraction of ice in a layered graphite, with comparable success (Gay *et al* 1992).

The influence of surface roughness on interfacial melting has been indicated in experiments on a glass substrate (Furukawa 1993), and convincingly demonstrated by studies with several modified glass surfaces (Beaglehole and Wilson 1994). Both studies used ellipsometry to gauge the thickness of the premelted layer. In the latter work no premelting was seen on smooth clean glass, but quite thick liquid-like films appeared on the same type of glass after roughening, at temperatures extending at least to  $-5\text{ }^{\circ}\text{C}$ , an effect termed *roughness-induced premelting*. The effect is an aspect of surface disorder, discussed earlier in this review. Beaglehole and Wilson (1994) also demonstrate *impurity-induced premelting*, by coating the glass substrate with a thin layer of NaCl before placing the ice on the glass.

### 3.3. Crystal growth

Because of the relevance to electronic materials, there is active research in crystal growth from the vapour. Many laboratory studies on other materials are of great importance for problems in atmospheric ice. The many forms of atmospheric ice have been thoroughly

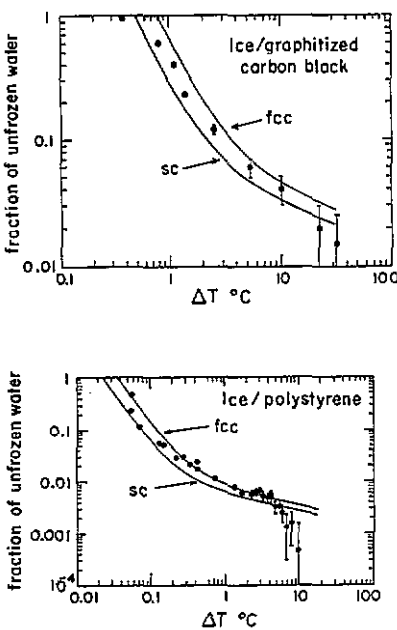


Figure 8. The fraction of unfrozen water in powders of monosized graphite (a) and polyethylene (b), compared to theoretical limits for surface melting and Gibbs-Thompson effect (Cahn *et al.* 1992).

treated by Hobbs (1974), and here we take a more narrow view. Since ice crystals act as substrates for many ozone degradation reactions it is of interest to pursue fundamental issues common to both natural and technical vapour growth.

While a great deal is known concerning interfacial structure at or near coexistence, the role of surface melting and disorder in the growth of crystals is, albeit fertile, still in its infancy (Bienfait 1992, van der Eerden 1993). Two relevant situations are surface roughening and surface melting. There is a substantial literature on *thermodynamic* roughening, wherein the height-height correlation length grows logarithmically with crystal size. Because of the change in the surface structure, this process has a profound influence on the local attachment kinetics, and ultimately on crystal shape. On isolated surfaces *thermodynamic* roughening and *kinetic* roughening (that resulting from imposition of a growth drive) have been extensively studied in systems such as He (Lipson and Polturak 1987, Balibar *et al.* 1993). The coexistence on a single crystal surface of different accretion mechanisms results in highly anisotropic growth (Frank 1958, and more recently Taylor *et al.* 1992, Elbaum and Wetlaufer 1993, Wetlaufer *et al.* 1994). In the case of surface melting, the communication with the parent phase is mediated by a mobile thin film. This should constrain the growth rate both by the difference in the vapour-solid and the vapour-liquid, liquid-solid accretion mechanisms, and the change in these with temperature as the film thickness changes. These variations of interfacial kinetics may be rate limiting. Löwen and Lipowsky (1991) find a dynamical thickening of the surface melt during evaporation, and related effects in the growth of ice from pure water vapour and in air can be found in Sei and Gonda (1989) and Elbaum *et al.* (1993).

#### 4. Non-equilibrium effects: thermomolecular pressure and transport

A thermomolecular pressure gradient associated with a temperature gradient produces the phenomenon known as 'frost heave' in moisture-containing porous media, e.g. frozen ground. But although frost heave is notorious in moist ground, thermomolecular pressure is a general phenomenon that can occur in any material. The basic requirement is a perturbed region of solid–liquid phase equilibrium extending over a span of temperatures, such as the thin liquid films coexisting with solid due to surface melting. There are several theoretical discussions of thermomolecular pressure from quite different viewpoints (Miller 1978, Gilpin 1980b, Derjaguin and Churaev 1986, Forland *et al* 1988, Dash 1989b, Wilen 1993). The following combines aspects of several treatments.

Referring to the discussion of surface melting in section 2.1, we note that the interfacial term in equation (2.4) is equivalent to a pressure difference  $\delta P_m = P_l - P_s$  between the melted layer and the solid. This results from the thermodynamic effect of a change in the external conditions on the chemical potential of a system. If the unperturbed chemical potential of a system is  $\mu(T, P)$  and the perturbation changes the energy per molecule by an amount  $u$ , the chemical potential is changed to

$$\mu'(T, P, u) = \mu(T, P) + u = \mu(T, P) + \delta P/\rho. \quad (4.1)$$

Hence the interfacial term introduces a pressure difference,

$$\delta P = P_l - P_s = \Delta\gamma(\partial f/\partial d) = \rho_l[(\mu_s)_{T,P} - (\mu_l)_{T,P}]. \quad (4.2)$$

At the transition temperature  $T_0$  of the bulk material,  $(\mu_s)_{T_0,P_0} = (\mu_l)_{T_0,P_0}$ , hence  $\delta P_m$  vanishes at  $T_0$ . However, the chemical potentials differ at  $T < T_0$ . With the expansion of  $\Delta\mu \equiv (\mu_s - \mu_l)$  to first order, as in equation (2.5), we obtain a general thermodynamic relation for the *thermomolecular pressure difference*:

$$\delta P = -\rho_l q_m t - (1 - \rho_l/\rho_s)(P_s - P_0). \quad (4.3)$$

Thus a temperature gradient induces a pressure gradient, which tends to drive the flow of the liquid layer. Two limiting cases of equation (4.3) are interesting. Liquid transport ceases when the liquid layer is at uniform pressure,  $P_l = P_0$ . Solving for the pressure in the solid then yields

$$P_s - P_0 = \rho_s q_m t. \quad (4.4)$$

In general, liquid transport causes a pressure build-up in the solid until the flow ceases. For water, this *maximum frost heave* pressure is approximately  $1.1 \times 10^6$  Pascals  $\text{deg}^{-1}$  (see table 1). It is the maximum pressure which can build up as a result of the flow of unfrozen water to the freezing front. When the pressure in the ice reaches this value, opposed by an equal pressure from the wall, the flow ceases. The pressure exerted on the ice by the wall is referred to as the *overburden pressure* and in soils is the result of the weight of ground above the ice front plus the cohesive strength of the soil. When there is no overburden pressure from the wall there will be a flow of water in the melted layer to the ice front. The water freezes there, heaving the wall up. We can find the pressure which drives the flow in the liquid layer by setting  $P_s = P_0$ :

$$P_l - P_0 = -\rho_l q_m t. \quad (4.5)$$

The pressure decreases for decreasing temperature, causing water to flow to the colder region. The negative sign reflects the fact that the interaction between the boundary surfaces of the melt liquid is equivalent to a 'disjoining pressure' which tends to thicken the liquid layer, but is opposed by the free energy of conversion of solid to liquid.

In the more general case when the overburden pressure is between  $P_0$  and the maximum pressure, the pressure in the melted layer can be expressed as follows:

$$P_1 - P_0 = -\rho_1 q_m t + \frac{\rho_1}{\rho_s} (P_s - P_0). \quad (4.6)$$

The flow is related to the 'thermomolecular pressure gradient' in the melted layer:

$$\nabla P_1 = \frac{\rho_1 q_m}{T_0} \nabla T + \frac{\rho_1}{\rho_s} \nabla P_s. \quad (4.7)$$

The theory has been broadened to include other causes of premelting, not only wetting forces (Dash 1992). It is shown that the effect can occur whenever phase equilibrium is perturbed such that premelted liquid coexists with solid. Liquid may exist at temperatures and pressures below the normal phase boundary for a variety of reasons: surface melting, capillarity, supercooling, surface disorder, solutes and confinement. When that occurs, a thermomolecular pressure will attend a temperature gradient in any material, regardless of its constitution.

The universality of the theory has been tested by experimental studies. Several measurements of the maximum frost heave pressure in frozen soils and other porous media have shown close agreement with the theory (Radd and Oertle 1973, Takashi *et al* 1981); examples of such results are given in figure 9. More recently, thermomolecular pressures have been measured in  $^4\text{He}$  solid in porous glass of several pore sizes (Hiroi *et al* 1989). In the He studies the temperature variations were in some cases so great that the thermomolecular pressure showed the effect of second-order terms in the expansion of the chemical potential; nevertheless, extremely close agreement with the theory was obtained.

Table 1 lists the maximum thermomolecular pressure coefficients for several materials, according to equation (4.4).

Table 1. Thermomolecular coefficients of various substances.

Substance	$T_0$ (K)	$dP_m/dT$ (bar K $^{-1}$ )
Argon	83	5.7
Gallium	292	2.6
Hydrogen ( $\text{H}_2$ )	13.8	3.2
Lead	600	4.5
Mercury	234	7.1
Water	273	11.2
Helium( $^4\text{He}$ )	4	2.4

To date, thermomolecular coefficients have been measured carefully in only two substances:  $\text{H}_2\text{O}$  and  $^4\text{He}$ , and the theoretical slope has been confirmed in both. There is no reason to doubt that similarly consistent results can be obtained with other substances, although two examples might be a rather slim basis for accepting a universal relation. However, there is a stronger motivation for extending such studies. The transport of very thin films should be influenced by the reduced fluidity due to the ordering imposed by

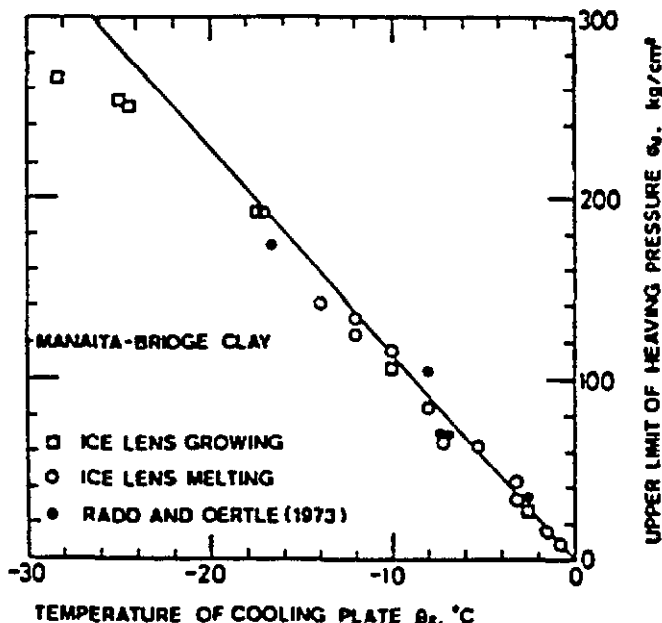


Figure 9. Measurements of the maximum frost heave pressures in soils, compared to theory (Takashi *et al* 1981).

close confinement. The thinness of liquid-like films due to surface and interfacial melting, together with the drive that can be provided by thermomolecular pressure gradients, offer unusually convenient means for studying the proximity effect.

The dynamics of thermomolecular flow and the magnitudes of pressure effects depend on the geometry as well as the temperature gradient. Two current studies are now exploring the detailed dynamics in simple systems.

An experimental study of thermomolecular pressure and flow on single facets of ice is under current study by Wilen and Dash (1994). The physical system, shown schematically in figure 10(a), consists of a thin cylindrical freezing cell, where ice can be grown in a radial temperature gradient, controlled so that the ice-water interface can be maintained at a fixed radius. The top face of the cell is a thin elastic membrane, which can stretch to conform to the local topology of the ice during growth. The evolution is monitored by interference microscopy and polarimetry (figures 10(b), (c)).

In a first principles calculation stimulated by the above investigation, Wettlaufer and Worster (1994) study the shape of an advancing ice interface in a deformable cylindrical channel. A temperature gradient along the channel produces a thermomolecular pressure gradient, which in turn causes the flow of premelted film toward lower temperature. To represent the response to freezing in some biological capillaries and other experimental systems, the cylinder walls are assumed to be elastic (figure 11).

## 5. Ice in the environment

Ice plays major roles in the thermal, chemical and biological processes of the natural environment. It exists in a variety of forms over a large part of the land area of the globe.

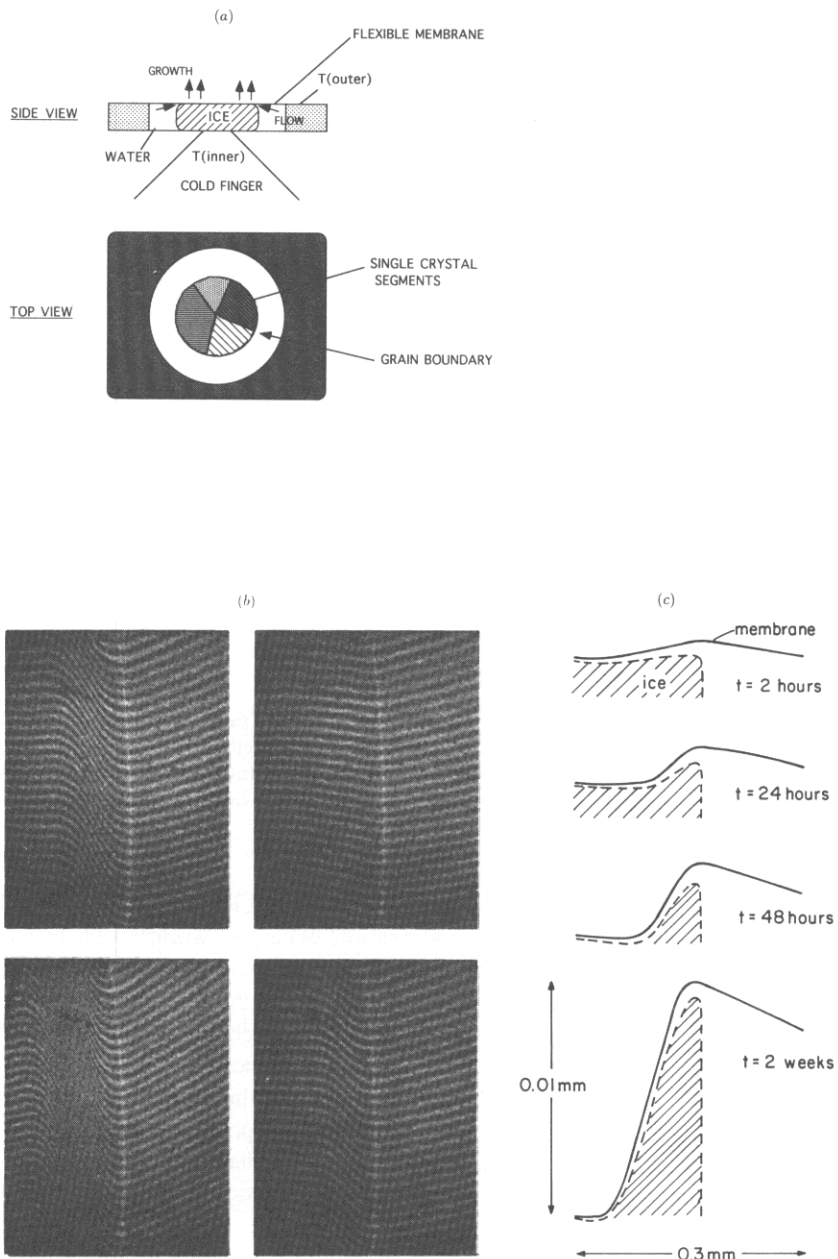


**Figure 10.** Experimental study of frost heave on single crystal facets of ice (Wilen and Dash 1994). (a) Cell and interference microscope. (b) Interferometry patterns after time intervals during thermomolecular pressure-driven flow along the interface between ice crystal and taut plastic membrane stretched over the ice. (c) Cross sections of the crystal deduced from the interferometry.

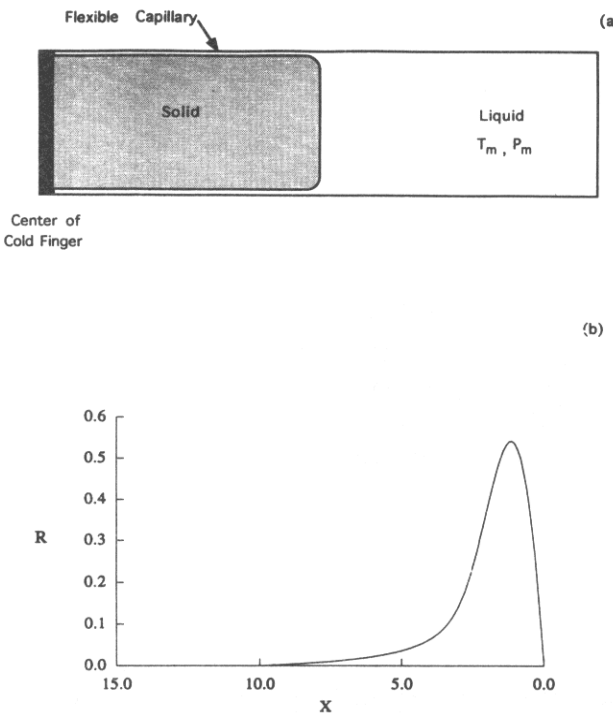


**Figure 11.** Theoretical study of frost heave of a single crystal contained in an elastic capillary. (a) Schematic of capillary, crystal and thin premelted annulus of liquid. The temperature at the centre of the cold finger is less than  $T_m$ , which drives thin film flow toward the centre. (b) The resulting dimensionless distortion of the elastic capillary walls during frost heave (Wettlaufer and Worster 1994).

Most of the Earth's pure water is in solid form, in glaciers and snow fields. The reflectivity of glaciers, snow fields and frozen oceans influences the world's heat balance and climate. The dynamics of freezing causes the breakdown of exposed rocks and damages engineered structures. The frost resistance of plant species limits their geographical spread. Permafrost contains great quantities of methane, a powerful greenhouse gas. The electrification of thunderstorms involves active ice formation. Ice particles in polar stratospheric clouds are reservoirs of ozone-destroying chemicals. In each of these processes, the phase equilibrium between ice and water is the basic thermodynamic process that governs the manner and importance of ice's involvement. In every case, the phase change at surfaces and interfaces produces distinctive characteristics which differ significantly from the bulk transition.

### 5.1. Friction; ice and snow

The slipperiness of snow and ice has been the basis for some of the oldest forms of transportation. Sleds and skis are still important today, although their practical use in cold regions is overshadowed by their popularity in winter sports. Less pleasurable are the difficulties that ice and snow present to other forms of transport, particularly automobiles and foot travel. These concerns have motivated research on snow and ice friction for many years. A recent bibliography of the subject (Colbeck 1993) lists more than 300 selected

articles dating from 1900, including over 30 in the past 3 years. Yet in spite of the long history of scientific attention, the nature of snow and ice friction is still not completely understood. The development of better practical surfaces, for lower friction in skiing and ice skating, and for higher friction in automobile tyres, continues to be actively researched today.

The coefficient of kinetic friction of ice can be orders of magnitude lower than that of most common materials. The minimum coefficient reported, under speed skating conditions, is 0.0046 at  $-7^{\circ}\text{C}$ . (De Koning *et al* 1992). The slipperiness of ice has prompted the common speculation that lubrication is supplied by a water film. Reynolds (1901) suggested that the film is due to pressure melting. But experiments on ice and snow by Bowden and Hughes (1939) showed that pressure melting might be a factor only at temperatures close to  $0^{\circ}\text{C}$  and at low speeds. If the sliding speed is appreciable and the temperature is more than a degree or so below the melting point, a lubricating film of meltwater can be produced by frictional heating. They showed that the electrical conductivity between two electrodes on the slider surface indicated the presence of a water film several tens of micrometres thick. The frictional heating due to the motion could account for the melting of a film of such thickness. Several studies since then confirm the importance of frictional heating (Bowden 1953, Evans *et al* 1976, Colbeck 1988, Colbeck and Warren 1991) but also that additional mechanisms play significant roles in snow friction. Colbeck (1988) has shown that the total friction in sliding on snow is composed of a combination of dry friction, ploughing, lubricated friction and capillary suction. Dry friction and ploughing are dominant at low film thickness, i.e. at low speed and low temperature. Lubricated friction, where the total coefficient is a minimum, occurs at intermediate thicknesses. Capillary suction, which is due to the adhesion of liquid to the slider, dominates at large thickness, primarily at temperatures close to  $0^{\circ}\text{C}$ . These factors in turn depend on several characteristics of the slider surfaces: thermal conductivity, hardness and hydrophilicity.

Static and kinetic friction coefficients at low speeds have similar values, and at temperatures well below the melting point the friction coefficient of ice is not greatly different from the coefficients of ordinary substances (Bowden 1953). Under these conditions, when lubricating films are absent sliding must involve deformation and fracture of asperities on the surfaces. Although meltwater films cannot be present below the melting point at very low speeds, there is evidence for film lubrication even under these conditions. Colbeck's theory predicts film thicknesses from 0.1 to 0.4  $\mu\text{m}$  for plastic and aluminium sliders over a  $40^{\circ}\text{C}$  temperature range. Since, in the case of complete surface melting, the film thickness diverges as the temperature approaches  $0^{\circ}\text{C}$ , the contribution to lubrication may be non-trivial.

Offenbacher *et al* (1973) measured the deformation and sliding resistance of a single crystal of ice against glass plate, for various loads and temperatures between  $-7.5$  and  $-19^{\circ}\text{C}$ . They proposed that the variation of friction with speed and temperature indicated creep or viscosity of a thin non-Newtonian interfacial layer. A strong decrease of resistance with temperature is consistent with our current understanding of interfacial melting. Quantitatively, however, their results disagree with recent measurements, since the temperature dependence of the friction was much more rapid than the usual power law; furthermore, there was a finite shear strength before sliding began. Another experimental study, published in the same year, gave qualitatively similar results. Barer *et al* (1977) measured the motion of an ice plug in a quartz capillary, driven by gas pressure. The results were interpreted in terms of an unfrozen viscoelastic layer having a finite shear strength. The layer thickness was calculated from nuclear magnetic resonance measurements of the water-ice fraction in a fine powder of silica spheres (see section 3.1). The calculated

viscosity was up to an order of magnitude greater than the viscosity of supercooled bulk water at the same temperature. In earlier measurements by some of the same investigators (Kvilividze *et al* 1974), the friction of ice on flat quartz surfaces was much higher, and was attributed to 'catching' of the ice by microscopic asperities. The discrepancies are probably due to differences in the sensitivity of the techniques to surface roughness. As pointed out by Barer *et al*, the sliding velocity of the ice column is sensitive to very small variations in the smoothness and diameter of the capillary tube.

Moreover, a study of wire regelation by Gilpin (1980a) gave no indications of a finite shear strength (see section 3.3). This was consistent with analysis of the dynamical equations, which showed that the motion was quite insensitive to roughness on the scale of the actual irregularities. Gilpin's measurements gave a higher viscosity than bulk values, but only at temperatures lower than  $-10^{\circ}\text{C}$ . As discussed earlier, such an increase might be due to a proximity effect in the very thin films.

In summary, the nature of friction on ice and snow varies with the conditions; principally of temperature and velocity. Water-lubricated friction exists at low velocity down to several degrees below  $0^{\circ}\text{C}$ ; of this range, pressure melting is typically limited to less than  $1^{\circ}$ , and interfacial melting at lower temperature. At lower temperature, a liquid film can be created by frictional heating due to high relative velocity. The state of the surface is important in all of the regions. The loading pressure and its time duration control the plastic deformation and recrystallization of the ice (Offenbacher *et al* 1973), affecting the area of contact. At temperatures close to the melting point pressure melting can cause major remoulding of the ice to the slider, tending to lock the two surfaces together. In thick films the wettability of the slider is important, as capillary forces can add considerably to the total drag force.

## 5.2. *Soil freezing, permafrost and frost heave*

### 5.2.1. *Soil freezing.*

5.2.1.1. *Ice in frozen soils.* Soils can be described as loosely bonded porous media, with pores of irregular shapes and sizes bounded by soil grains. In moist soils at subzero temperatures, ice can exist in a variety of forms, principally of two types. The first, called 'pore ice', has crystallite sizes of the same order as those of the soil particles. Pore ice tends to cement soil grains together, accounting for the typically great increases in the strength of frozen ground.

The second main category of ice has much larger sizes, ranging from millimetres to metres. Such segregated ice can result from different processes, leading to distinctive characteristics. Pingos are large, ice-cored mounds formed by water under pressure (Washburn 1973, MacKay 1988), the water having originated from thawed regions, and then been trapped by freezing from above. Ice wedges are formed from periodic thermal expansion and contraction of frozen ground, where cracks are filled with meltwater during the warmer seasons. Foliated ice consists of lenses, sheets ranging in thickness from hairline streaks to metres, generally oriented parallel to the ground surface. They originate from unfrozen water drawn from nearby moisture sources or premelts of nearby ice, especially 'pore ice', to the freezing front, due to thermomolecular pressure gradients (see section 3). The particular form of ground ice is determined by the local soil structure, its moisture content, solute concentration, overburden, and the local and non-local history of temperature and temperature gradient.

*5.2.1.2. Melting of ice in soils.* Ice in frozen ground melts at temperatures below the bulk transition due to a combination of surface melting, impurities and curvature effect (see section 2.3). Unfrozen water films exist at ice interfaces with the soil particles or at grain boundaries (section 2.2) well below 0 °C. The fraction of unfrozen water is determined by the sizes and shapes of the ice crystals, impurity concentrations and the local environment (Reed *et al* 1979). The unfrozen water fraction against temperature, or soil freezing curve (SFC), is commonly used to quantitatively describe the water content in a frozen soil (figure 12).

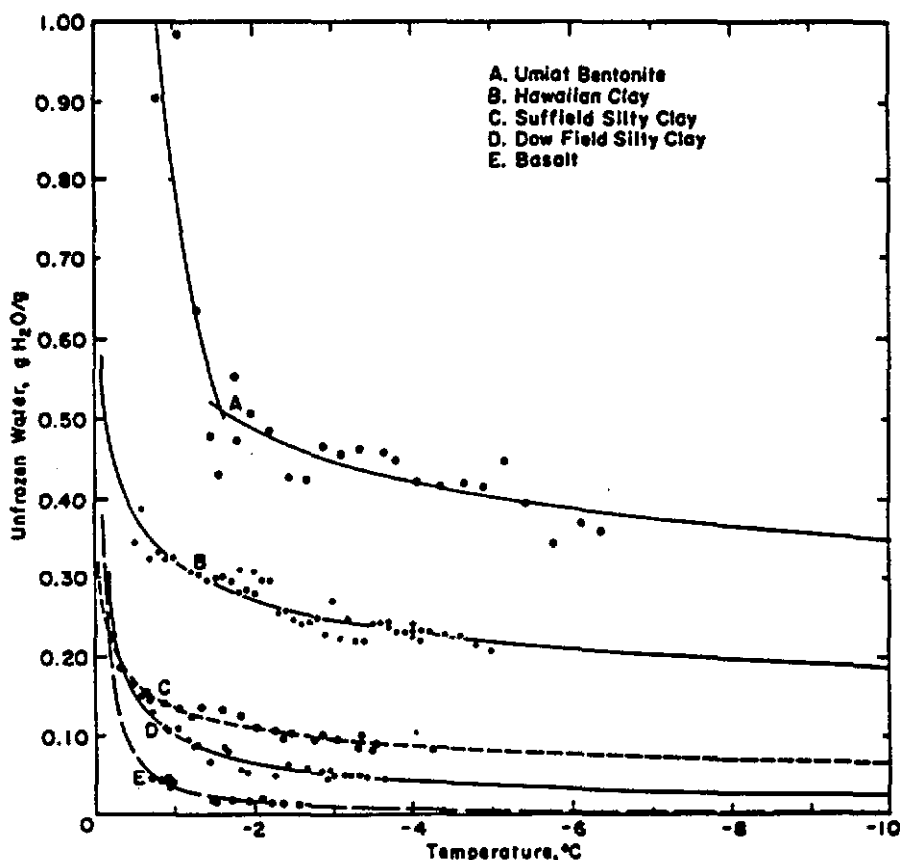


Figure 12. Soil freezing curves; the unfrozen water in various soils as a function of temperature (Anderson and Tice 1973).

By measuring the volumetric change with temperature by use of a dilatometer, Bouyoucos and McCool (1916) demonstrated the existence of liquid water in subfreezing soil for the first time. Since Bouyoucos's pioneering work, calorimetry has been used as one of the main techniques to determine SFCs (Nersesova 1953, Kolaian and Low 1963, Anderson and Tice 1973). The different response or relaxation times of the magnetic dipole moments of protons and the electrical dipole moments of water molecules in liquid water and solid ice, under excitation by external electromagnetic fields, provide two fruitful techniques: nuclear magnetic resonance (NMR) and time domain reflectometry (TDR), both of which offer accurate quantitative measurements of water content. Introduced by Tice *et*

*al* (1978) to measure SFCs, NMR has proven to be a reliable method (Isizaki *et al* 1990, Tice *et al* 1988). Recently, NMR has been employed by Overloop and van Gerven (1993) to study the adsorbed water in high surface area materials, observing surface water layers persisting to very low temperature.

In TDR (Fellner-Feldegg 1972), an electromagnetic pulse is applied to a sample with characteristic frequency in the range 10 MHz to 5 GHz, where the dielectric properties of ice and water differ dramatically. The travel time of the pulse in a fixed length of the soil column is used to calculate the dielectric constant of the bulk sample (e.g. Smith and Tice 1988), from which the unfrozen water content can be deduced either from an empirical formula (Topp *et al* 1980) or from other more sophisticated models (Hanai 1968). More careful treatment of the TDR data necessitates studies of the incident and reflected pulses in the frequency domain (Patterson and Smith 1980, Delaney and Arcane 1984). The SFCs obtained measured by TDR and NMR were found to be consistent, as shown by Smith and Tice (1988).

Other techniques used to measure the water content in the frozen media include acoustic methods (Timur 1968, Rong *et al* 1983, Deschates *et al* 1988) and neutron scattering (Dore *et al* 1987, Maruyama *et al* 1992, Gay *et al* 1992). By considering the interface properties of the ice–water–substrate combination, the freezing curves may be deduced from other related phenomena, including surface area measurements (Anderson and Tice 1972), water condensation (Black and Tice 1989) and mercury porosimetry (Fu and Dash 1993).

In the field, *in situ* unfrozen water fraction can be measured by modified TDR equipment (Zegelin *et al* 1989) or by directly employing electromagnetic pulses at VHF or higher frequencies. Signal delay times and amplitudes from the emitter to the receiver embedded in the frozen ground are measured (Arcane and Delaney 1989). Some geophysical properties, such as the dielectric constants and attenuation rates of frozen ground, can be deduced, though the technique requires further improvements.

It is not possible to calculate the SFC of soil from fundamental properties due to the complexity of the structure and chemistry of soil. An alternative method of predicting the SFC has been developed by Fu and Dash (1993). The method was developed and tested with powders of monosized spherical particles and the water fraction was found to be consistent with a quantitative theoretical prediction, discussed earlier in section 3.3. In the case of heterogeneous powders and soils, mercury intrusion was shown to be a surrogate for the SFC. Rather than attempting to obtain a detailed profile of the pore size distribution, the SFC was obtained by a simple scaling of the mercury intrusion volume versus pressure data.

**5.2.2. Permafrost.** Permafrost, ‘permanently frozen ground’ (Muller 1947), refers to ground that is frozen for long periods of time. Permafrost covers about 20% of the Earth’s surface and extends to the subpolar regions. The vertical extent of permafrost ranges from a fraction of a metre to hundreds of metres. The temperature of the permafrost at depths of several metres from the ground surface remains as a constant roughly equal to the annual average of the local atmospheric temperature. Permafrost may involve not only land areas, but also seabed sediments (Gosink and Baker 1990). Many studies have been devoted to the impacts of permafrost, especially its deformation, on natural resources and human constructions (Cooley 1990, Permafrost 1988, 1993).

**5.2.2.1. Active layer.** Above the permafrost is the active layer (Muller 1947), a layer of ground that freezes and thaws seasonally or daily. The thickness of the active layer ranges from a tenth to several metres, depending on the local climate, type of surface exposure,

composition of the ground, hydrology and vegetation. Damage is imposed on landscapes and engineered structures mostly by the active layer through *frost action*. The frost heaving process will be discussed in section 5.2.3.

**5.2.2.2. Permafrost and climate.** Regional climatic variation may substantially impact the state of permafrost (Harrison 1991). Climate variation cycles the temperature of the active layer above the permafrost (e.g. Muller 1947, Delaney 1987). Ice lenses or wedges form during winter and melt when the seasonal temperature rises. After repeatedly freezing and thawing, especially combined with frost action, the mechanical strength of the frozen ground is degraded (Vialov 1965) due to the loosened soil textures, which can lead to the deformation of the landscape, erosion and sediment production (e.g. Akan 1984, Cooley 1990).

The global climate affects the permafrost and *vice versa* (e.g. Anisimov 1990). Thawing permafrost can release greenhouse gases, thus possibly promoting global warming and thereby accelerating the release (reviewed by Nisbet 1989). The principal culprit is methane, stored as methane-ice clathrates, which are stable at depths of greater than about 200 metres in the permafrost (MacDonald 1990). The release is believed to have the potential for an appreciable effect on the climate-permafrost system (Nisbet 1990, Sommerfeld *et al* 1993).

**5.2.2.3. Solutes and frozen ground.** Solutes redistribute in freezing soils, due to partial exclusion from the ice phase and transport due to thermomolecular pressure gradients. The redistribution can be significant for agricultural chemicals, both fertilizers and insecticides (Cooley 1990). Solutes may also migrate in frozen soils, by diffusion through the unfrozen water or vapour. The migration is affected by local chemistry, temperature variations, surface homogeneity (Thompson 1991) and relative size of the solute molecules with respect to the size of the migration channel. The osmotic potential resulting from the increased solution concentrations during freezing will contribute to the water migration, promoting frost action (Cary 1987, Kadlec *et al* 1988). Impurities may also crystallize from a highly concentrated solution, inducing a local dilution to cause more impurities to migrate to the vicinity. As a result, the local soils will be degraded due to the high salinity. With high salinity, 'salt heave' may emerge as an important heave-driving force (Chen *et al* 1989).

### 5.2.3. Frost action in soils, rocks and concrete.

**5.2.3.1. Frost heave in soils.** Frost heave is a non-equilibrium process, consisting of heat and water transport, ice formation and ground deformation. Typical conditions leading to frost heave in the natural environment are shown in figure 13. The basic forcing mechanism is the thermomolecular pressure due to a temperature gradient (described in section 4), which causes a flow of premelted liquid toward lower temperature. In subzero weather the unfrozen water migrates through the ground toward the surface, and is replenished by soil moisture from lower, warmer levels. With continued inflow the local pressure increases, until it exceeds the soil's cohesive strength and overburden, causing the ground to rupture. The liquid that enters the cavity begins to freeze, since its melting point is that of the bulk phase, rather than that of the pore liquid. While the *ice lens* grows, fed by the inflow, it lifts the surface of the ground. As the freezing level penetrates further into the ground, the local temperature at the lens falls, and so does the flow rate, due to the decreasing fraction of unfrozen water (the soil freezing curve). Then the inflowing water begins to accumulate some distance below the lens, and the process of pressure build-up and soil rupture occurs

in a new region below the first. In this manner, a heaving soil typically develops a series of thin layers of ice, oriented parallel to the surface. A number of theoretical papers have described the overall process, the most successful being Gilpin's (1980b). (Note, however, that the effects of curvature alone have been put forth to explain frost damage (Everett 1961).)

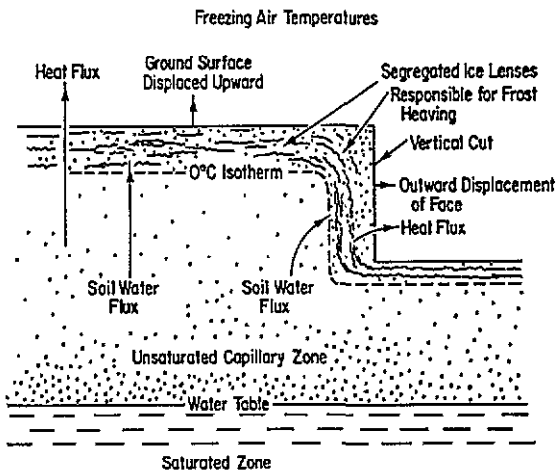


Figure 13. Typical conditions of frost heave and ice segregation in the natural environment (Polar Research Board 1984).

The theoretical maximum frost heave pressure for  $\text{H}_2\text{O}$ , listed in table 1, has been verified in several measurements on various soils (see figure 9), and the results are consistent with the prediction that the maximum pressure is completely independent of the nature of the medium. However, the dynamics of frost heave, which involves thermophysical, fluid dynamic, thermodynamic properties and mechanical behaviours of the frozen ground, is not well understood. Considerable work continues on dynamical aspects of frost heave, by laboratory studies, in-field investigations and theoretical modeling (Sayward 1979, Ishizaki and Nishio 1988, Fowler 1989).

The thermal conductivity of the frozen ground is determined by the properties of soil (mineralogy and particle sizes) and the volumetric fraction of ice and unfrozen water (Nakano and Horiguchi 1985, Gravril'ev 1989). The thermal conductivity of unfrozen water ( $\sim 0.58 \text{ W} (\text{Km})^{-1}$ ) is several times smaller than that of ice ( $\sim 2.3 \text{ W} (\text{Km})^{-1}$ ). Therefore growth of ice enhances the thermal conductivity and promotes ice growth. The preferential growth direction lies along the freezing isotherm.

Unfrozen water is transported through the melted surface layer (e.g. Deryagin and Churaev 1980, Wilen and Dash 1994, Wettlaufer and Dash 1994) or through regelation (O'Neill and Miller 1985). Water migration through soils has been studied both theoretically (Nakano and Horiguchi 1985) and experimentally (Mageau and Morgenstern 1980, Perfect and Williams 1980, Nakano and Tice 1988). The role of the vapour phase cannot be simply neglected. D'Orazio *et al* (1989) tested the self-diffusion of water in porous silica glasses with various filling fractions of water and found that the self-diffusion along the substrate surface is greatly enhanced by the fast interphase exchange between vapour and liquid.

Ice segregation is the determinant process in frost action and its rate, combined with the heat transfer rate, is often used as the index of the frost susceptibility of a soil. Ice

segregation has been studied by growing ice from water through a very thin capillary (Vignes and Dijkema 1974, Biermans *et al* 1978) and through microporous membranes (e.g. Ozawa and Kinoshita 1989). The local temperature at the ice front is found to be crucial to the segregation while the remote temperature is not. The hydraulic pressure and heaving pressure are found to be closely related to the segregation (Miller *et al* 1960, Buil *et al* 1982), and this plays an important role in a detailed theory of lens formation (Gilpin 1980b). The experiments confirm the observations that ice segregation occurs most frequently in fine-grained soils, such as clays and silts, where large unfrozen water content exists (Muller 1947). An intermediate temperature exists where the frost heave activity is maximized (Hallet *et al* 1991), due to the compromise between the rate of heaving pressure build-up (decreasing as  $T$  falls due to slowing water migration) and its absolute value (increasing as  $T$  falls).

The soil overburden and external loading may reduce the ground heave and the internal strength of soil may also slow down the heave action, as seen in the slow fracture of rocks (Hallet *et al* 1991). On the other hand, at low temperature (below  $-10^{\circ}\text{C}$ ), ice formed through segregation will strengthen the frozen ground by cementing soil particles (Muller 1947). With regard to other mechanical behaviours of frozen soils, readers are referred to the review by Sayles (1988).

Various theoretical models of frost heave have been proposed and simulations have been based on these considerations. Detailed processes in frost heave were explored in these models, including ice lensing, internal pressure of freezing soil, heave amplitudes, and solute effects for both saturated and unsaturated conditions (O'Neill and Miller 1985, Padilla and Villeneuve 1992).

**5.2.4. Rock deformation by frost action.** The deformation of rock at low temperature is now believed to be primarily due to frost heave rather than to the expansion of water on freezing. The volume increase due to the water–ice phase transition during initial freezing of moisture has minimal effects on rocks (Walder and Hallet 1985), considering that excess water in the cracks can be expelled due to the relatively rigid structure of rock. At a moderately low temperature ( $-5$  to  $-10^{\circ}\text{C}$ ), frost heave pressure builds up in the rock pores through ice segregation and eventually is strong enough to produce microcracks, whose growth leads to deformation and breakage. When the temperature is lowered further, the amount and mobility of unfrozen water decreases and the activity of rock breakage diminishes as the build-up of frost heave pressure slows down. Progress in this field has been reviewed by Hallet *et al* (1991). Similar processes can lead to degradation of exposed concrete structures.

**5.2.5. Food preservation.** Frost action is involved in food preservation by freezing. The ice in frozen foods may segregate due to temperature variation during storage and transport (e.g. Martino and Zaritzky 1989, Wetlaufer and Worster 1994). The size modification of ice microcystallites may alter the food texture and, by puncturing cell walls, allow fluids to escape, thereby reducing its nutritional value. A full understanding of the segregation of ice is also important to the cryopreservation of organic tissues for medical purposes (Foreman *et al* 1993, Tourtellotte *et al* 1993).

**5.2.6. Upfreezing of rocks and patterned ground.** Frozen ground forms patterns under periodic seasonal or diurnal freezing and thawing cycles (Washburn 1980, Hallet 1990a, Krantz 1990). Stones and fine-grained soil particles are sorted to form either circles or polygons on horizontal ground or stripes on hillslopes (see figure 1). Generally found in

the high mountains of temperate zones and in remote locations far beyond the tree-line in the Arctic and Antarctic, the patterns have sizes ranging from a few centimetres to metres.

Patterned ground forms by particles being sorted according to their sizes so as to alter the soil density profile (Hallet 1987). The movements of the particles at different locations of the patterned ground has been mapped by Hallet (1987), who observed an intermittent circulation in stone circles on Spitzbergen Island, pictured in figure 1. The mechanism propelling the soil particles is still under debate. In a free convection model described by Krantz and his coworkers (Krantz 1990), the water convects due to an unstable water density profile established during summer warming. Mathematical simulations based on this model predict the geometrical dimensions observed in the field (e.g. George *et al* 1989, McKay 1992), but the driving force necessary to cause the soil movement appears too weak to account for the observed motion. Another convection model proposed by Hallet and his coworkers (1990a) assumes larger density variations, those resulting from uneven moisture distribution due to thawing and consolidation. This model is also able to predict the geometric dimensions of the sorted ground pattern. However, the soil dynamics have not been studied in either of these models.

### 5.3. Glaciers, sea ice and snow fields; sintering and sliding

**5.3.1. Glaciers.** The decay of glacier ice and the distribution of chemicals in deep ice cores are two issues of importance to climate change. There are two broad categories of glacier ice: *temperate* and *polar*. Temperate polycrystalline ice exists at  $T \approx T_0$ , and contains a finite liquid volume fraction, and polar ice is 'cold' and 'dry'. The process of 'ice decay' or 'ice rotting' is sensitive to the volume and distribution of intraglacial liquid (Nye 1991, 1992). Liquid can be present as the result of precipitation or leaching of impurities, interfacial energy effects, in internal melt-figures, called Tyndall figures, and at interior interfaces associated with air and/or water-vapour bubbles, among others. Raymond and Harrison (1975) have observed such liquid in temperate glacier ice. The high DC conductivity observed in cold polar ice has been ascribed to the lack of internal liquid mobility as compared to temperate ice, and thus the inability of polar ice to flush impurities (Wolff and Paren 1984). Impurity redistribution in glacier ice may be of crucial importance in the climate analyses of ice cores (Souchez and Lorrain 1991) although isotope glaciologists have yet to investigate many premelting phenomena.

At temperatures near  $T_0$  polycrystalline ice can contain liquid water due solely to the impurity and curvature depressions of the freezing point (e.g. Nye 1992). This water resides at tri-grain junctions in microscopic channels (10–100  $\mu\text{m}$ ) called *veins* and at *nodes* separating four grains, so that a given sample may be able to communicate liquid throughout its volume (figure 14). Assuming that the interfacial coefficients are *independent* of crystallographic orientation, Nye and Frank (1973) predicted this geometrical network. It can be understood by considering a trijunction where three grains abut (figure 14). On balancing the interfacial coefficients, the dihedral angle  $2\theta_0$  is determined by the simple ratio

$$2 \cos \theta_0 = \gamma_{ss} / \gamma_{sl}. \quad (5.1)$$

Thus, the node shape and vein cross section depend only on this ratio of surface energies, and water enters the grain boundary groove at an angle  $2\theta_0$ . Mader (1992a) observed  $2\theta_0$  ranging from  $25^\circ$  to  $105^\circ$ , but typically between  $30^\circ$  and  $40^\circ$ . Of course, this implies that the grain boundary is not wet by the liquid phase. This question could be studied using neutron diffraction or time domain reflectrometry as discussed above. In two dimensions

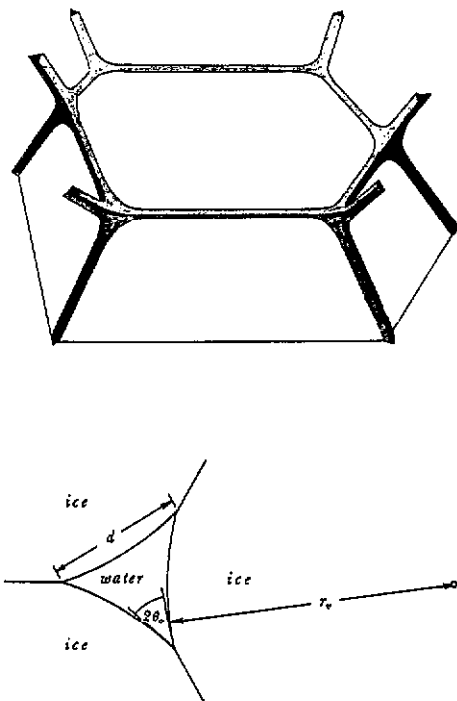


**Figure 14.** A schematic of the *vein-node* system in polycrystalline ice (modified from Nye 1989). The upper diagram depicts the *veins* at a triple-grain junction, and the *nodes* where four veins and hence four grains intersect. The bottom diagram is a cross section of a vein showing the dihedral angle. For ice near the melting point, such a network can be responsible for the communication of liquid throughout the volume of the sample.

it is a general result (Cahn 1991) that two-phase trijunction angles are determined by the ratio of the  $\gamma$ s, as in equation (5.1). Grain boundaries can become unstable to wetting and be replaced by two interfaces.

Nye (1989) computed the detailed shape of an isolated node for  $2\theta_0 = 33.6^\circ$ . The nodes have regular tetrahedral symmetry, and the veins have three-fold symmetric cross sections. The theoretical prediction for the variation of vein size with temperature has been verified experimentally by Mader (1992b). Nye (1992) has reviewed the relevant experiments, theory and application of his continuum thermal evolution theory to glaciers. Because of its general applicability to annealing, and importance in ‘ice rotting’, we describe his calculation below.

Consider a circular area, of radius  $r_e$ , equivalent to that of the vein cross section (figure 14), and veins of uniform impurity concentration. The melting point depression of a polycrystal of given vein geometry can be expressed as

$$\delta T = \frac{A}{r_e} + \frac{B}{r_e^2} \quad (5.2)$$

where for  $2\theta_0 = 25^\circ$ ,  $A = 54.4 \text{ \AA K}$  and  $B = mc/\pi$  with  $m$  the liquidus slope and  $c$  the impurity concentration per unit vein length. During the cooling of a polycrystal near  $T_0$ , the vein volume decreases and impurities are rejected by the ice to enrich the liquid.

The freezing point due to both curvature and impurity concentration is lowered so that further cooling is retarded. In bulk, this has the effect of an anomalous heat capacity of a value greater than that of pure ice. Because of its dependence on vein area, when  $r_e$  is small, the impurity term dominates in the determination of the equilibrium temperature until  $\delta T \approx 10^{-5}$  K, below which the curvature term becomes important. For an initially uniform vein impurity concentration, the difference in the mean curvature between the surface and the interior of a sample results in a lower melting point in the interior. Internal melting occurs as the sample equilibrates and the liquid fraction increases. Nye (1991, 1992) calls this process 'rotting', and uses it to model the boundary between temperate and polar ice. Mader (1992b) has taken into consideration the mass transport due to volume contraction on melting, and obtains excellent agreement with the experimental data; veins can grow in width by  $\approx 1$  mm in 100 days.

In the same review, Nye points out that under normal pressures liquid lenses are observed to form along the grain boundaries themselves. Because of their (outward) convexity, their equilibrium temperature is higher than surrounding regions, and they eventually freeze.

The approaches discussed above treat two ingredients of the recent studies of polycrystalline ice in contact with monosized powders (Cahn *et al* 1992), but do not treat the issue of grain boundary melting due to structural mismatch, as discussed in section 2.2. These effects would come into equation (5.2) with a stronger  $r_e$  dependence, but with a very small coefficient, and so may only be acting at temperatures of interest in polar glaciers. Another glaciological problem with roots in the 'wire regelation' studies mentioned previously concerns the mechanics of glacial basal sliding. Among other things, it depends on the bulk water permeability and melting between basal rock and ice (e.g. Alley 1993). Finally, Nye has noted the geometrically similar two-phase network present in the Earth's mantle (Frank 1968). Hence, transport of the liquid phase of mantle material due to both the issues discussed in this section and thermomolecular pressure gradients may be relevant in understanding the Earth's structure and evolution.

**5.3.2. Sea ice.** Roughly one half the surface heat loss during the Arctic winter derives from latent heat release during solidification. This contributes about a sixth of the radiative loss to space (Peixoto and Oort 1992). Hence, solidification accounts for a substantial portion of the winter atmospheric energy budget. One of the polar oceans is freezing on any given day.

A review of the growth and structure of naturally occurring sea ice can be found in Weeks and Ackley (1986) and Wettlaufer and Weeks (1995), but a brief introduction is in order here. During winter, cracks in the perennial sea ice cover expose the ocean ( $T \approx -2$  °C) to a relatively cold ( $T \approx -30$  °C) atmosphere. A surface skim of the ocean is slightly undercooled so that the ice crystals (supplied by the local snowcover) that enter the water grow by dissipation of latent heat into the surrounding fluid. The strong growth anisotropy in ice (the rapid growth direction being perpendicular to the crystallographic *c* axis) results in disc-shaped crystals with axis parallel to the *c* axis and perpendicular to the water-air interface. Due to capillary waves on the water surface, the floating crystals coalesce at various angles from vertical, allowing some to grow into the fluid more rapidly than others. In the absence of severe mechanical agitation, a transition from vertical to horizontal *c*-axis orientation is observed within the top few centimetres of the ice cover (figure 15). Ice growth proceeds by molecular attachment to the existing solid. Initially, a small region the size of an individual grain (of order 1 cm) has a macroscopically smooth interface, but a lamellar/cellular interface forms as freezing progresses. Mature Arctic sea ice has a substructure consisting of horizontal *c* axes, with random intergrain orientation. Vertical

pure ice platelets extend into the water, and separate regions of highly concentrated seawater (figure 15). The substructure has a scale (fractions of a millimetre) set by the competition between the solutal and thermal diffusion fields and interfacial surface tension, but theory predicts that the onset of the cellular instability will be difficult to determine experimentally (Wettlaufer 1992). This is primarily due to the strong impurity segregation (cf section 2.6) between ice and aqueous solutions, an effect with similar consequences in alloy growth (Mullins and Sekerka 1963). As the ice sheet grows downward, the substructure is embedded in the material and secondary instabilities result in the formation of isolated brine inclusions, which can be viewed as 'negative crystals'. Therefore, at every level sea ice is a mixture of pure ice and concentrated seawater. Hence, the phase transition on a coarse scale is continuous rather than first order.

Figure 15 displays the high crystallinity of sea ice, its spatial variation and that of the liquid fraction. Unfrozen solution exists in the bulk inclusions, created by the interfacial growth instability, both within single crystals and at grain boundaries, in veins and at nodes. As the material thickens it cools, but the temperature gradient continually changes, and the grains coarsen with depth. The transient temperature gradient drives continuous freezing and impurity diffusion, so that an inclusion migrates toward warm temperatures, i.e. toward the bottom of the sea ice. This is one of several mechanisms of sea ice desalination (Knight 1967, Untersteiner 1968), with downward rates of 5 to  $2500 \mu\text{m h}^{-1}$  (Hoekstra *et al* 1965, Jones 1974) which make the process more important in the internal redistribution of impurities. The latter, primarily through the control of liquid fraction, determines the anomalous thermal conductivity, heat capacity and *effective* latent heat of sea ice (Schwertfeger 1963). Since these properties determine the bulk thermal diffusivity of the material, they play an obvious role in the perennial growth and decay of sea ice.

Interesting interfacial effects are found experimentally, but much of the underlying mechanisms remain unconfirmed. Jones (1974) observed ten classes of inclusion shapes, and concluded that both the shape and the migration direction were related to the crystallography of the surrounding ice. He also found that the migration direction was not always parallel to the temperature gradient. In addition, there were faceting shape transitions and transient events, some of which were associated with migration along grain boundaries. In contrast, Hoekstra *et al* (1965) concluded that no such crystallographic dependence was operative. While Jones' experiments suggest strong kinetic and interfacial effects, he found no agreement with kinetic models. We are unaware of more recent studies covering the same range of conditions.

The major salt in seawater is NaCl, but the phase diagram is quite complicated. Once the temperature decreases below the eutectic for a particular salt, an individual inclusion (or fraction of it) will precipitate. Interfacial melting, at the solid-salt/ice interface, allows the continued migration of the salt crystal toward warmer temperatures. Evidence of this was found by Hoekstra *et al* (1965), who observed the migration of KCl crystals at temperatures below the eutectic point.

The grain boundary phase changes and crystallographic re-orientation in naturally occurring sea and glacier ice are analogous to grain growth and coarsening in many materials. The theory for the stability and evolution of grains in polycrystals does not consider the effect of premelted liquid (Cahn 1991). In a temperature gradient, grain growth mediated by premelting and curvature effects will result in a spatially variable grain network. The kinetics of motion will depend on whether the interface separates the same or different phases, a problem that has not been investigated and is relevant both in sea and glacier ice.

An active experimental and theoretical field considers the solidification of systems in which the resulting 'solid' has a large liquid fraction, as in sea ice. This phase change

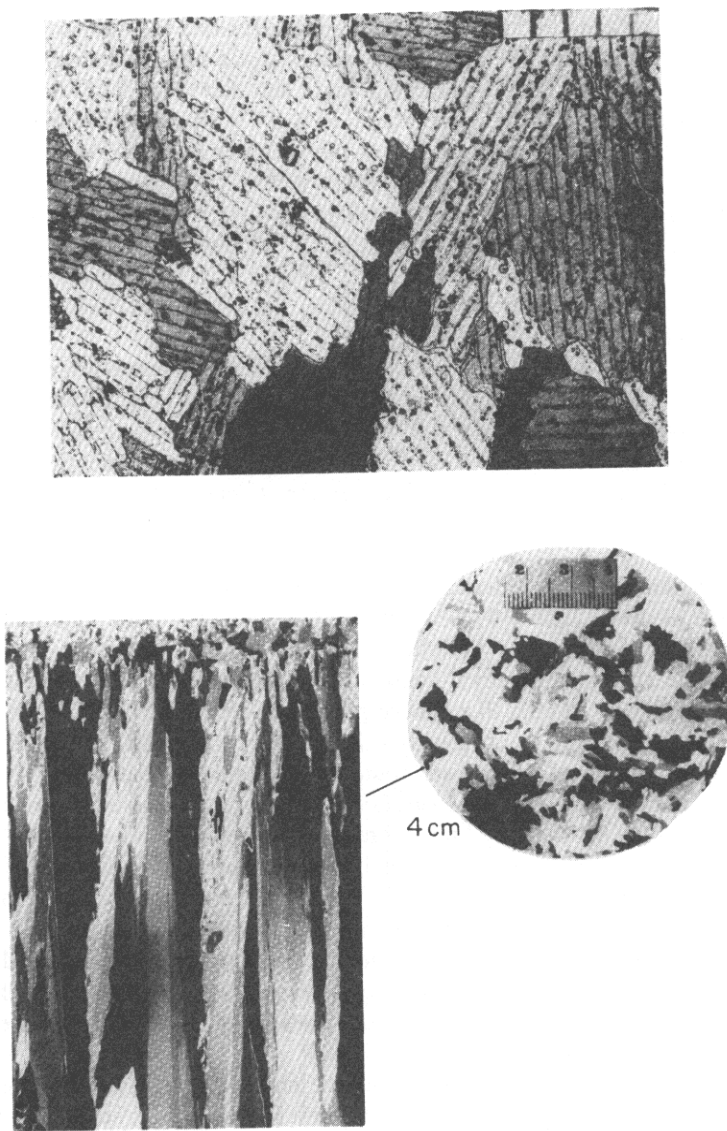


**Figure 15.** Thin sections of sea ice as viewed under crossed polarizers, where the different shades distinguish individual crystals. The top diagram is a horizontal section, and the dark linear features are highly concentrated seawater within each crystal and along crystal boundaries. This cellular structure is the result of a growth instability (see text). The bottom diagram is a 12 cm vertical thin section with a horizontal slice taken at 4 cm in the circular region. Note the grain coarsening with depth. The smallest subdivisions in the scale are millimetres. After Gow *et al* (1987).

process can be accompanied and/or controlled by hydrodynamic interactions. Examples in other areas include vacuum arc welding or melting, laser-controlled zone refining and ingot quenching (e.g. Langer 1992), crystallization in magma chambers and lava lakes (Huppert 1990, Worster 1992).

**5.3.3. Snow fields; sliding and sintering.** Most of the northern hemisphere is covered by snow during winter. The structure and dynamics of snow can effect our work, recreation skiing, drinking water and transportation, among a myriad of other things. Since snow often exists close to the melting temperature, it may undergo substantial evolution due to mass transport induced by gradients in temperature, pressure, water content and grain curvature (Colbeck 1982). This redistribution of mass exerts an influence on the seasonal layering of snow, and can result in notable problems such as avalanches. Faraday's observation (section 1.1) of the relative ease of making a snowball when the temperature is near 0 °C is related to the ready *sintering* of ice crystals. While sintering and related snow metamorphosis problems are of importance in the stability of snow fields, it is also crucial in the metallurgy of powders (Herring 1964).

The basic mechanism of sintering is well understood (Herring 1964). One observes that when two ice particles are put in contact at a point, and the contact force is removed, the area between the particles increases in time. The concavity at the contact point implies a large cost in free energy, and if a reduction in free energy can be accommodated by the transport of material, a neck will form between them. Depending on the experimental conditions, there are many mechanisms by which the mass transfer can occur (e.g. Herring 1964, Hobbs 1974): diffusion (a) through the background vapour, (b) over the crystal surfaces and (c) through the bulk solid, and also material deformation. While these are plausible and some have a sound experimental basis, the role of a surface melted layer is yet to be thoroughly assessed. If a layer of liquid exists at the crystal surface, there is a ready and mobile medium through which the transport can occur. Indeed, the evidence of an enhancement of surface melting on ice in contact with air (Elbaum *et al* 1993) suggests its importance for snow morphology. Colbeck (1982, 1993) has brought sintering and other surface thermodynamic concepts to bear on a myriad of problems in snow metamorphism, and we refer the reader to his work for treatments in depth.

#### 5.4. Atmospheric ice

**5.4.1. Thunderstorms.** Lightning is one of Nature's most spectacular phenomena. It has evoked wonder and awe in all cultures, and it has been a focus of scientific attention for centuries. As a result, we now know a great deal about the structure and dynamics of thunderstorms and their electrical discharges. And yet the fundamental mystery, the mechanism that generates the charging, is still unexplained. But what is known is relevant to this review: that, in the opinion of most atmospheric scientists, the charge separation mechanism involves ice (Fleagle and Businger 1980, Latham 1981, Williams 1988).

The typical structure of most thunderclouds is shown in figure 16. The source of most of the lightning strokes that reach the ground is a region of negative charge density. The major portion of the cloud's positive charge is in the upper reaches, while a smaller fraction lies near the cloud bottom. The negative region contains supercooled drops, vapour-grown ice crystals and a kind of soft hail called graupel, which are agglomerations of ice grains and freezing supercooled water droplets. The ice crystals are formed where strong updrafts of moist air are cooled to temperatures well below 0 °C. As the air rises and cools, fine ice particles are nucleated and carried upward at speeds that can exceed several metres per second. Considerable evidence from laboratory experiments suggest that charge separation occurs during collisions between the fine ice particles and the graupel (Buser and Aufdermaur 1977, Gaskell and Illingworth 1980, Jayaratne *et al* 1983, Caranti *et al* 1985, Baker *et al* 1987, Keith and Saunders 1988). The magnitude and polarity of the charge transfer depend on the temperature, the supercooled liquid water content of the cloud, the impact velocity and the growth rates of the particles. Laboratory measurements show that

the collision process is sufficiently powerful to account for the charging rate in thunderstorms (for example, Caranti *et al* 1985), but the basic cause of the charge separation in collisions is not known. A number of theories have been proposed over the years, involving electrostatic induction (Wilson 1929), freezing potentials (Workman and Reynolds 1948), thermoelectric effects (Latham 1961), deformation and fracture (Takahashi 1983, Williams 1985, 1990, Beard and Ochs 1986, Caranti *et al* 1991), evaporation and growth (Dong and Hallett 1992), and surface melting (Turner and Stow 1984, Baker and Dash 1989, 1994). No model as currently formulated satisfies all of the observations, but surface melting appears to provide a framework for explaining many features.

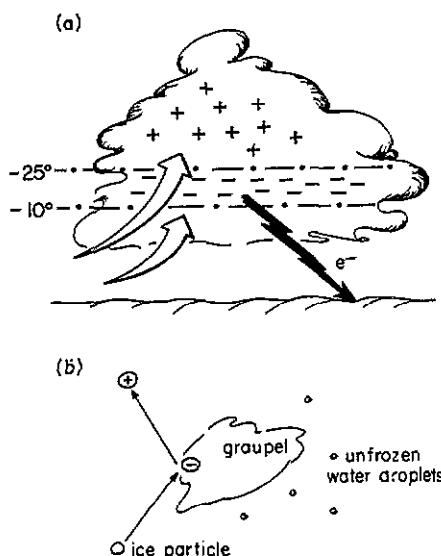


**Figure 16.** (a) The structure of a typical thunderstorm, showing the origin of lightning in a negatively charged zone near the cloud bottom, and the principal region of positive charge at higher elevations. (b) Schematic showing the charging attendant on inelastic collisions between fine ice particles and graupel (soft hail), believed to be the principal mechanism of charge separation in thunderstorms.

The involvement of surface melting in charge transfer was first suggested by the observation that temperatures in the zone of cloud electrification are within the range expected for surface melting of ice (Turner and Stow 1984). Baker and Dash (1994) have proposed a detailed charging mechanism, which is a consequence of mass transfer between colliding particles having surface melted films of differing thickness. The liquid is charged due to differential adsorption of positive and negative ions at the liquid-ice interface, neutralized by a diffuse layer of oppositely charged ions in the adjacent liquid. Such double charge layers are common at the interfaces between water and mineral surfaces. The characteristic Debye length of the diffuse distribution in water depends on the ion concentration, but is in all probability much greater than the very thin layers of interest here. Therefore, the charge density extends throughout the thickness of surface melted films at several degrees below 0 °C. In a typical encounter between an ice particle and graupel, the contacting surface films will have different thicknesses due to different growth rate, temperature and curvature. During a collision liquid will flow from the thicker to the

thinner film, driven by the tendency for their chemical potentials to equalize. Since the outer layers of film carry a net excess of ions of one type, charge is automatically transferred along with the mass transfer.

Quantitative estimates indicate that the theoretical mechanism can provide a magnitude of charge transfer comparable to observed rates in thunderclouds.

Regardless of the theory under test, further comparisons and predictions will require more detailed experimental investigations, particularly of the microscopic character of the ice particles and their surfaces, their dependence on environmental conditions, and correlations with the sign and magnitude of charge transfer.

**5.4.2. Atmospheric chemistry.** The discovery of an 'ozone hole' over Antarctica in late austral winter and early Spring (Farman *et al* 1985) and, more recently, a weaker deficit appearing over the Arctic, has led to considerable research on the processes responsible. It is now known that polar stratospheric clouds (PSCs) play a crucial role in the destruction of O<sub>3</sub> in the winter and spring months (Koehler *et al* 1993, Molina 1993).

The most important reaction involving the cloud particles is



This reaction converts inert chlorine (in ClONO<sub>3</sub>, HCl) into photochemically active Cl<sub>2</sub>. The cloud particles act as reservoirs and meeting grounds of the reagents, thereby raising their reaction rates. One of the foremost current questions is the identification of the accommodation mechanism.

The cloud particles are principally of two types: type I consists of nitric acid trihydrate crystals (NAT), which form at temperatures several degrees above the frost point of water, and type II, particles composed primarily of water ice. The quantities of chemicals stored by the particles are much greater than can be accommodated by adsorption; on the other hand, the partitioning of HCl between liquid and solid phases indicates that very little can be dissolved in the solid interior of the particles. Consequently, it has been proposed that the HCl is dissolved in multilayer-thick quasi-liquid films (Abbatt *et al* 1992). Measurements indicate that solute-stimulated surface melting can produce sufficiently thick quasi-liquid layers to dissolve very large quantities of the reagent chemicals (Lamb and Blumenstein 1987, Conklin 1993), although the amount of liquid required may be much greater than can be explained by surface melting (Baker and Dash 1994).

The scavenging of pollutants in the lower atmosphere involves issues similar to those of ozone destruction. It is known that soluble and insoluble compounds are scavenged from the atmosphere by rain or snow, but the processes of incorporation are still under study. Candidate mechanisms include sorption in cloud droplets and raindrops, adsorption on snow crystals and incorporation into snow by nucleation or impaction (Mitra *et al* 1990, Conklin 1993). The importance of snow crystals as scavengers has been seen in field studies, where they contributed about twice as much to the removal of sulphate as did rain (Murukami 1983). Laboratory measurements have investigated the various mechanisms, particularly surface and growth processes (Lamb and Blumenstein 1987, Valdez and Dawson 1989, Mitra *et al* 1990). On the basis of these and other studies, it appears that the efficiency of snow scavenging is due to absorption in liquid-like surface layers during growth, at temperatures as low as -15 °C (Clapsaddle 1989, Abbatt *et al* 1992).

## Acknowledgments

We are grateful to J P D Abbatt, M B Baker, B Hallet, J F Nye and L Wilen for their careful reading of the manuscript and very valuable criticisms and suggestions and to W F Weeks

for encouraging our work on sea ice. This work has been supported in part by National Science Foundation grants DPP9023845 and DMR 9220729, and Office of Naval Research grants ONR N00014-90-J-1369 and N00014-94-1-0120.

## References

- Abbatt J P D et al 1992 *J. Geophys. Res.* **97** 15819-26
- Abraham F F 1981 *Phys. Rep.* **81** 339-74
- Akan A O 1984 *Water Resources Res.* **20** 707-13
- Alley R B 1993 *J. Glaciol.* **39** 447-54
- Amaya K et al 1987 *Japan. J. Appl. Phys.* **26** Suppl 26-3, CK01
- An G and Schick M 1989 *Phys. Rev. B* **40** 9722-5
- Anderson D M and Morgenstern N R 1973 *Permafrost. Proc. 2nd Int. Conf.* (Washington, DC: National Academy of Science) pp 257-88
- Anderson D M and Tice A R 1972 *Highway Res. Record* **393** 12
- 1973 *Ecological Studies* vol 4 (Berlin: Springer) p 107
- Anisimov O A 1989 *Sov. Meteorol. Hydrol.* **1** 65
- 1990 *Sov. Meteorol. Hydrol.* **3** 32
- Arcone S A 1984 *Geophysics* **49** 10 1763
- Arcone S A and Delaney A J 1989 *CRREL Report 89-4* (Cold Regions Research and Engineering Laboratory, Hanover, NH)
- Aziz M J 1982 *J. Appl. Phys.* **53** 1158-68
- Baker B, Baker M B, Jayaratne E R, Latham J and Saunders C P R 1987 *J. R. Meteorol. Soc.* **113** 1193-215
- Baker G C and Osterkamp T E 1988 *Proc. 5th Int. Symp. on Ground Freezing* ed R H Jones and J T Holden (Rotterdam: Balkema) pp 29-33
- Baker M B and Dash J G 1994 *J. Geophys. Res.* **99** 10621-6
- 1989 *J. Cryst. Growth* **97** 770-6
- Balibar S, Edwards D and Laroche C 1979 *Phys. Rev. Lett.* **42** 782-5
- Balibar S, Gallet F, Gruner F and Rolley E 1993 *Prog. Cryst. Growth Char. Mat.* **26** 51-66
- Banin A and Anderson D M 1974 *Water Resources Res.* **10** 124
- Barer S S et al 1977 *Dokl. Akad. Nauk USSR* **235** 601-3
- Bar-Ziv R and Safran S A 1993 *Langmuir* **9** 2786-8
- Beaglehole D 1991 *J. Cryst. Growth* **112** 663-9
- Beaglehole D and Nason D 1980 *Surf Sci.* **96** 357-65
- Beaglehole D and Wilson P 1994 *J. Phys. Chem.* **98** 8096-102
- Beamish J R, Hikata A, Tell L and Elbaum C 1983 *Phys. Rev. Lett.* **50** 425-30
- Beard K and Ochs H 1986 *The Earth's Electrical Environment; Studies in geophysics* (Washington, DC: National Academy Press)
- Bienfait M 1991 *Phase Transitions in Surface Films* vol 2, ed H Taub et al (New York: Plenum)
- 1992 *Surf Sci.* **272** 1-9
- Biermans M B G M, Dijkema K M and De Vries D A 1976 *Nature* **264** 166
- 1978 *J. Hydrol.*, Amsterdam **37** 137
- Binh V H and Melinon P 1985 *Surf Sci.* **161** 234-44
- Black P B and Hardenberg M J 1991 *CRREL Special Report 91-23* (Cold Regions Research and Engineering Laboratory, Hanover, NH)
- Black P B and Tice A R 1989 *Water Resources Res.* **25** 10 2205
- 1990 *Proc. Int. Symp. on Frozen Soil Impacts on Agricultural, Range, and Forest Lands* ed K R Cooley, p 54
- Blumberg R L, Stanley H E, Geiger A and Mausbach P 1984 *J. Chem. Phys.* **80** 5230-41
- Bouyoucos G J 1917 *Michigan Agr. Exp. Sta. Tech. Bull.* **36**
- Bouyoucos G J and McCool M M 1916 *Michigan Agr. Exp. Sta. Tech. Bull.* **24** p 592
- Bowden F P 1953 *Proc. R. Soc. A* **217** 462-78
- Bowden F P and Hughes T P 1939 *Proc. R. Soc. A* **172** 280
- Bowden F P and Tabor D 1964 *The Friction and Lubrication of Solids Part II* (Oxford: Clarendon)
- Brewer D F, Dahm A J, Hutchins W S and Williams D N 1978 *J. Physique* **39** C6-351
- Brewer D F, Rajendra J, Sharma N and Thomson A L 1990 *Physica* **165**, 166 569
- Bronshteyn V L and Chernov A A 1991 *J. Cryst. Growth* **112** 129-45
- Broughton J Q, Bonissent A and Abraham F F 1981 *J. Chem. Phys.* **74** 4029

- Broughton J Q and Gilmer G H 1983a *J. Chem. Phys.* **79** 5119–27  
— 1983b *Acta Metall.* **31** 845–51  
— 1986 *Phys. Rev. Lett.* **56** 2692–5
- Budyko M I, Izrael Yu A and Yanshin A L 1991 *Meteorologiya i Gidrologiya* **12** 5
- Buffat P and Borel J P 1976 *Phys. Rev. A* **13** 2287–98
- Buil M and Aguirre-Puente J 1981 *Winter Ann. Mtg Am. Soc. Mech. Eng.: Heat Transfer Div.*
- Buil M, Aguirre-Puente J and Soisson A 1991 *C.R. Acad. Sci. Paris* **293** 653–61
- Buser O and Aufdermaur A N 1977 *Electronic Processes in the Atmosphere, Proc. 8th Int. Conf. Atmos. Electr.* ed R Dolezalek (Darmstadt: Steinkopf) pp 294–301
- Cahn J W 1991 *Acta Metall.* **39** 2189–99
- Cahn J W, Dash J G and Fu H Y 1992 *J. Cryst. Growth* **123** 101–8
- Cahn J W and Kikuchi R 1985 *Phys. Rev. B* **31** 4300–4
- Caranti G, Avila E and Re M 1991 *J. Geophys. Res.* **96** 15365–75
- Caranti J M, Illingworth A J and Marsh S J 1985 *J. Geophys. Res.* **90** 6041–6
- Carnevali P, Ercolelli F and Tosatti E 1987 *Phys. Rev. B* **36** 6701–4
- Cary J W 1987 *Water Resources Res.* **23** 1620
- Chan M H W Private communication
- Chen X B, Qiu G Q, Wang Y Q, Sheng W K, Tao Z X and Tian L X 1989 *Science in China A* **32** 234
- Chernov A A 1993a *Prog. Cryst. Growth Mat.* **26** 195–218  
— 1993b *Prog. Cryst. Growth Mat.* **26** 121–51
- Chernov A A and Mikheev L V 1989 *Physica A* **157** 1042–58
- Colbeck S C 1982 *Rev. Geophys. Space Phys.* **20** 45–61  
— 1988 *J. Glaciol.* **34** 78–86 — 1991 *J. Glaciol.* **37** 228–35  
— 1992 *CRREL Report 92-2* (Cold Regions Research and Engineering Laboratory, Hanover, NH)  
— 1993 *CRREL Report 93-6* (Cold Regions Research and Engineering Laboratory, Hanover, NH)
- Colbeck S C and Warren G C 1991 *J. Glaciol.* **37** 228–35
- Conklin M H and Bales R C 1993 *J. Geophys. Res.* **98** 16851–5
- Cook J C 1960 *AIEE Trans. Pap.* **60** 994
- Cooley K R (ed) 1990 *Proc. Int. Symp. on Frozen Soil Impacts on Agricultural, Range, and Forest Lands. CRREL Report 90-1* (Cold Regions Research and Engineering Laboratory, Hanover, NH)
- Curtin W A 1987 *Phys. Rev. Lett.* **59** 1228
- D'Orazio F, Bhattacharja, S, Halperin W P and Gerhardt R 1989 *Phys. Rev. Lett.* **63** 43
- Dal Corso A and Tosatti E 1993 *Phys. Rev. B* **47** 9742–50
- Dash J G 1975 *Films on Solid Surfaces* (New York: Academic)  
— 1982 *Phys. Rev. B* **25** 508–12  
— 1989a *Contemp. Phys.* **30** 89–100  
— 1989b *Science* **246** 1591–4  
— 1990 *J. Cryst. Growth* **100** 268–70  
— 1991 *Phase Transitions in Surface Films* vol 2 ed H Taub *et al* (New York: Plenum) pp 339–56  
— 1992 *J. Low Temp. Phys.* **89** 277–81
- de Gennes P J G 1985 *Rev. Mod. Phys.* **57** 827–63
- De Koning J J, De Groot G and Van Ingen Schenau G 1992 *Biomechanics* **25** 565–71
- Delaney A J 1987 *CRREL Report 87-7* (Cold Regions Research and Engineering Laboratory, Hanover, NH)
- Delaney A J and Arcone S A 1984 *Cold Regions Science and Technology* **9** 39
- den Nijs M 1988 *Phase Transitions and Critical Phenomena* vol 12, ed C Domb and J Lebowitz (New York: Academic) pp 219–333
- Deryagin B V and Churakov N V 1980 *Kolloidnyi Zh.* **42** 842–52  
— 1986 *Cold Regions Science and Technology* **12** 57
- Deschrates M H, Cohen-Tenoudji F and Aguirre-Puente and Khastou 1988 *Proc. 5th Int. Conf. on Permafrost* vol 1, ed K Senneset (Trondheim: Tapir) p 324
- Dietrich S 1988 *Phase Transitions and Critical Phenomena* vol 12, ed C Domb and J Lebowitz (New York: Academic) p  
— 1993 *Phys. Scr. T49* 519–24
- Dietrich S and Napiorkowski M 1990 Private communication
- Dong Y and Hallett J 1992 *J. Geophys. Res.* **97** 20361–71
- Dore J C, Dunn M and Chieux P 1987 *J. Physique* **48** C1–457
- Dzyaloshinskii I E, Lifshitz E M and Pitaevskii L P 1961 *Adv. Phys.* **10** 165
- Elbaum M, Lipson S G and Dash J G 1993 *J. Cryst. Growth* **129** 491–505
- Elbaum M and Schick M 1991a *Phys. Rev. Lett.* **66** 11713–16

- 1991b *J. Phys. I, France* **1** 1665–8
- Elbaum M and Wetzlaufer J S 1993 *Phys. Rev. E* **48** 3180–3
- Evans D C B, Nye J F and Cheeseman K J 1976 *Proc. R. Soc. A* **347** 493–512
- Evans R 1979 *Adv. Phys.* **28** 143
- 1990 *J. Phys.: Condens. Matter* **2** 8989–9007
- Everett D H 1961 *Trans. Faraday Soc.* **57** 1541–51
- Faraday M 1850 *Lecture before the Royal Institution reported in The Athenaeum* no 1181, 640–1 — 1933 *Michael Faraday's Diary* (London: Bell and Sons) pp 79–81
- Farman J C, Gardiner B G and Shanklin J D 1985 *Nature* **315** 825–8
- Feder J, Russell K C, Lothe J and Pound C M 1966 *Adv. Phys.* **15** 111
- Fellner-Feldegg H R 1972 *Hewlett Packard Application Note* no 153
- Fionova L K and Artemyev A V 1993 *Grain Boundaries in Metals and Semiconductors* (Paris: Les Editions de Physique)
- Fleagle R G and Businger J A 1980 *An Introduction to Atmospheric Physics* 2nd edn (New York: Academic)
- Fletcher N H 1968 *Phil. Mag.* **18** 1287
- 1970 *The Chemical Physics of Ice* (Cambridge: Cambridge University Press)
- Foreman J, Moriya H and Taylor M J 1993 *Transpl. Int.* **6** 191–200
- Forland K S, Forland T and Ratkje S K 1988 *Irreversible Thermodynamics* (New York: Wiley) pp 235–44
- Fowler A C 1989 *SIAM J. Appl. Math.* **49** 991–1008
- Franck J P, Kornelson K E and Manuel J R 1983 *Phys. Rev. Lett.* **50** 1463–5
- Frank F C 1958 *Growth and Perfection of Crystals; Proceedings* ed R H Doremus, B W Roberts and D Turnbull (New York: Wiley)
- 1968 *Nature* **220** 350–2
- Franks F (ed) 1982 *Water: A Comprehensive Treatise* vol 7 (New York: Plenum)
- Frenkel J 1946 *Kinetic Theory of Liquids* (Oxford: Oxford University Press)
- Frenken J W M, Toennies J P and Wöll Ch 1988 *Phys. Rev. Lett.* **60** 1727–1730
- Frenken J W M and van der Veen J F 1985 *Phys. Rev. Lett.* **54** 134
- Fu H Y and Dash J G 1993 *J. Coll. Interface Sci.* **159** 343–8
- Fuoss P H, Norton L J and Brennan S 1988 *Phys. Rev. Lett.* **60** 2036
- Furukawa Y 1993 Private communication
- Furukawa Y, Koneki A, Yamamoto M and Kuroda T 1988 *J. Cryst. Soc. Japan* **30** 279–85
- Furukawa Y, Yamamoto M and Kuroda T 1987 *J. Cryst. Growth* **82** 665
- Gaskell W and Illingworth A J 1980 *Quart. J. R. Meteor. Soc.* **106** 841–54
- Gay J M, Suzanne J, Dash J G and Fu H Y 1992 *J. Cryst. Growth* **125** 33–41
- George J H, Gunn R D and Straughan B 1989 *Geophys. Astrophys. Fluid Dyn.* **46** 135
- Gibbs J W 1906 *Scientific Papers, vol 1: Thermodynamics* (London: Longmans Green and Co); reissued 1961 (New York: Dover) pp 219–52
- Gilpin R R 1979 *J. Coll. Interface Sci.* **68** 235–51
- 1980a *J. Coll. Interface Sci.* **77** 435
- 1980b *Water Resources Res.* **16** 918–30
- Gleason K J, Krantz W B, Caine N, George J H and Gunn R D 1986 *Science* **232** 216–20
- Goldthwaite R P 1976 *Quaternary Res.* **6** 27–35
- Golecki J and Jaccard C 1978 *J. Physique* **39** C11–4229
- Gosink J P and Baker G C 1990 *J. Geophys. Res.* **95** (C6) 9575
- Goto S, Shibuya M, Nakajima T and Kuroda M 1988 *Proc. 5th Int. Symp. on Ground Freezing* vol 1, ed R H Jones and J T Holden (Rotterdam: Balkema)
- Gravril'ev R I 1989 *Inzhenerno-Fizicheskii Zh.* **56** 995
- Gross G W, Gutjahr A and Caylor K 1987 *J. Physique* **48** C 527–33
- Gross G W, Wong P M and Humes K 1977 *J. Chem. Phys.* **67** 5264–74
- Häkkinen H and Landman U 1993 *Phys. Rev. Lett.* **71** 1023–6
- Häkkinen H and Manninen M 1992 *Phys. Rev. B* **46** 1725–42
- Hallet B 1976 *J. Glaciol.* **17** 209
- 1987 *Irreversible Phenomena and Dynamical Systems Analysis in Geosciences* ed C Nicolis and G Nicolis (Dordrecht: Reidel) pp 533–53
- 1989 Encyclopaedia Britannica Yearbook of the Future pp 86–97
- 1990a *Can. J. Phys.* **68** 842–52
- 1990b *Earth Sci. Rev.* **29** 57–75
- 1993 *Nature* **361** 142–5

- Hallet B, Anderson S P, Stubbs C W and Gregory E C 1988 *Proc. 5th Int. Conf. on Permafrost* ed K Senneset (Trondheim: Tapir) p 770
- Hallet B, Walder J S and Stubbs C W 1991 *Permafrost and Periglacial Processes* 2 283
- Hanai T 1968 *Emulsion Science* ed P Sherman (New York: Academic) pp 353–496
- Harrison W D 1991 *J. Geophys. Res.* 96 (B1) 683
- Herring C 1964 *Physics of Powder Metallurgy* ed W E Kingston (New York: McGraw-Hill)
- Heyraud J C and Métois J J 1987 *J. Cryst. Growth* 82 269–73
- Hiroi M, Mizusaki T, Tsuneto T, Hirai A and Eguchi K 1989 *Phys. Rev. B* 40 6581
- Hobbs P V 1974 *Ice Physics* (Oxford: Clarendon)
- Hoekstra P and Miller R D 1967 *J. Coll. Interface Sci.* 25 166–73
- Hoekstra P, Osterkamp T E and Weeks W F 1965 *J. Geophys. Res.* 70 5035
- Huppert H E 1990 *J. Fluid Mech.* 212 209
- Ishizaki T and Nishio N 1988 *Proc. 5th Int. Symp. on Ground Freezing* vol 1, ed R H Jones and J T Holden (Rotterdam: Balkema) pp 65–72
- Isizaki T, Fukuda M and Hirano A 1990 *Low Temp. Sci. A* 50 69
- Israelachvili J N 1992 *Intermolecular and Surface Forces* (New York: Academic)
- Jackson C L and McKenna G B 1990 *J. Chem. Phys.* 93 9002–11
- Jaworowski Z, Segalstad T V and Hisdal V 1992 *Norsk Polarinstitutt Meddelelser* 119 1
- Jayanthi C S, Tosatti E and Pietronero L 1985 *Phys. Rev. B* 31 3456–9
- Jayarathne E R 1991 *Atmos. Res.* 26 407–24
- Jayarathne E R, Saunders C P R and Hallett J 1983 *Quart. J. R. Meteor. Soc.* 109 609–30
- Jones D R H 1974 *J. Cryst. Growth* 26 177
- Kadlec R H, Li S M and Cotten G B 1988 *Water Resources Res.* 24 219
- Karim O A, Kay P A and Haymet A D J 1990 *J. Chem. Phys.* 92 4634–5
- Kay B D and Groenevelt P H 1983 *4th Int. Conf. on Permafrost* (Washington, DC: National Academy of Science) p 584
- Kay B D and Perfect E 1988 *Proc. 5th Int. Symp. on Ground Freezing* vol 1, ed R H Jones and J T Holden (Rotterdam: Balkema) pp 3–21
- Keith W D and Saunders C P R 1988 *Proc. Int. Conf. Atmos. Elect.* pp 282–7
- Ketcham W M and Hobbs P V 1969 *Phil. Mag.* 19 1161
- Keys J G, Johnston P V, Blatherwick R D and Murcay F J 1993 *Nature* 361 49–51
- Khalil M A K and Rasmussen R A 1989 *Tellus ser B: Chem. Phys. Meteor.* 41B 554
- Kikuchi R and Cahn J W 1980 *Phys. Rev. B* 21 1893–7
- Kisileva O A and Sobolev V D 1980 *J. Coll. Interface Sci.* 74 173
- Knight C A 1967 *The Freezing of Supercooled Liquids* (Princeton, NJ: Van Nostrand) — 1971 *Phil. Mag.* 23 153
- Koehler B G, McNeill L S, Middlebrook A M and Tolbert M A 1993 *J. Geophys. Res.* 98 10563–71
- Kofman R et al 1993 Private communication
- Kolaian J H and Low P F 1963 *Soil Sci.* 95 376
- Kondo Y, Kodama Y, Hirayoshi Y, Misuzaki T, Hirai A and Eguchi K 1987 *J. Appl. Phys. Suppl.* 26 303–6
- Koopmans W R and Miller R D 1966 *Proc. Soil Sci. Soc. Am.* 30 680
- Kozlowski T 1989 *Frost in Geotechnical Engineering* vol 1 (Finland: Saariselka) p 283
- Krantz W B 1990 *Earth Sci. Rev.* 29 117–30
- Krim J and Chiarello R 1991 *J. Vac. Sci. Technol. B* 9 2566–9
- Krim J, Coulomb J P and Bouzidi J 1987 *Phys. Rev. Lett.* 58 583–6
- Kristensen J K and Cotterill R M J 1977 *Phil. Mag.* 36 437
- Kuroda T 1985 *Proc. 4th Int. Symp. on Ground Freezing, Sapporo* — 1987 *J. Physique* 48 C1–487
- 1990 *J. Cryst. Growth* 99 83–7
- Kuroda T and Lacmann R 1982 *J. Cryst. Growth* 56 189
- Kvilividze V I, Kisilev V F, Kurzaev A B and Ushakova L A 1974 *Surf. Sci.* 44 60
- Lachenbruch A H 1962 *Geol. Soc. Am. Special Paper* 70
- Lamb D and Blumentstein R 1987 *Atmos. Environ.* 21 1765–72
- Landau J, Lipson S G, Määttänen L M, Balfour L S and Edwards D O 1980 *Phys. Rev. Lett.* 45 31–4
- Landau J and Saam W F 1977 *Phys. Rev. Lett.* 38 23–6
- Langer J S 1992 *Phys. Today* 45 24
- Latham J 1981 *Quart. J. R. Meteor. Soc.* 107 277–98
- Latham J and Mason B J 1961 *Proc. R. Soc. A* 260 523–36
- Lee R E Jr, Costanzo J P, Davidson E C and Layne J R Jr 1992 *J. Thermal Biol.* 17 263

- Lied A, Dosch H and Bilgram J H 1994 *Phys. Rev. Lett.* **72** 3554–7
- Liezhao C, Brewer D F, Girit C, Smith E N and Reppy J D 1986 *Phys. Rev. B* **33** 106
- Lipowsky R 1982 *Phys. Rev. Lett.* **49** 1575
- Lipowsky R and Speth W 1983 *Phys. Rev. B* **28** 3982
- Lipson S G and Poltak E 1987 *Prog. Low Temp. Phys.* **11** 128–88
- Low P F 1976 *Soil Sci. Soc. Am.* **40** 500
- 1979 *Soil Sci. Soc. Am.* **43** 651
- 1980 *Soil Sci. Soc. Am.* **44** 667
- Löwen H 1994 *Phys. Rep.* **237** 249–324
- Löwen H, Beier T and Wagner H 1989 *Europhys. Lett.* **9** 791
- Löwen H and Lipowsky R 1991 *Phys. Rev. B* **43** 3507–13
- MacDonald G J 1990 *Climatic Change* **16** 247
- Mackay R 1988 *Can. J. Earth Sci.* **25** 495–511
- Mader H 1992a *J. Glaciol.* **38** 333–47
- 1992b *J. Glaciol.* **38** 359–74
- Mageau D W and Morgenstern N R 1980 *Can. Geotech. J.* **17** 54
- Malton I 1988 *Logistics Today* **7** (4) 25–7
- Martino M N and Zaritzky N E 1989 *Cryobiology* **26** 138–48
- Maruyama M 1989 *J. Cryst. Growth* **94** 757–61
- Maruyama M, Bienfait M, Dash J G and Coddens G 1992 *J. Cryst. Growth* **118** 33
- Maruyama M, Bienfait M, Liu F C, Liu Y M, Vilches O E and Rieutord F 1993 *Surf. Sci.* **283** 333–7
- Mazzega E, del Pennino U, Loria A and Mantovani S 1976 *J. Chem. Phys.* **64** 1028–31
- McKay G 1992 *Proc. R. Soc. A* **438** 249–63
- Métois J J and Heyraud J C 1989 *J. Physique* **50** 3175
- Miller R D 1978 *Proc. 3rd Int. Conf. on Permafrost, NRC, Ottawa, Canada* vol 1, pp 707–13
- Miller R D, Baker J H and Kolaian J H 1960 *7th Int. Congr. Soil Sci. Trans.* vol 1 122
- Mitra S K, Barth S and Pruppacher H R 1990 *Atmos. Environ. A* **24** 2307–12
- Mizuno Y and Hanafusa N 1987 *J. Physique* **48** C1–511
- Molina M 1993 *Chemistry of the Atmosphere: The Impact of Global Change* ed J G Calvert (Oxford: Oxford University Press)
- Molz E and Beamish J R 1992 *Bull. Am. Phys. Soc.* **37** 125
- Mulla D J and Low P F 1983 *J. Coll. Interface Sci.* **95** 51
- Muller S W 1947 *Permafrost or Permanently Frozen Ground and Related Engineering Problems* (Ann Arbor, MI: J W Edwards Inc)
- Mullins W W and Sekerka R F 1963 *J. Appl. Phys.* **34** 323–9
- Nakano Y 1990 *Cold Regions Sci. Technol.* **17** 207
- Nakano Y and Horiguchi 1984 *Adv. Water Resources* **7** 93
- 1985 *Adv. Water Resources* **8** 50
- Nakano Y and Takeda K 1991 *Cold Regions Sci. Technol.* **19** 225
- Nakano Y and Tice A R 1988 *Proc. 5th Int. Conf. on Permafrost* vol 1 ed K Senneset (Trondheim: Tapir) p 412
- National Research Council Canada 1989 *Glossary of Permafrost and Related Ground-Ice Terms* Permafrost Subcommittee on Geotech. Res. Tech. Mem. 142
- Nenow D 1984 *J. Cryst. Growth Charact.* **9** 185
- Nenow D and Trayanov A 1986 *J. Cryst. Growth* **79** 801
- 1989 *Surf Sci.* **213** 488–501
- 1990 *J. Cryst. Growth* **99** 102–5
- Nersesova Z A 1953 *Akademika Nauk SSSR, Materialy Po Laboratornym Issledovaniyam Merzlykh Gruntov SB-1*
- Nguyen T, Ho P S, Kwok K, Nitta C and Yip S 1986 *Phys. Rev. Lett.* **57** 1919–22
- Nisbet E G 1989 *Can. J. Earth Sci.* **26** 1603–11
- 1990 *Can. J. Earth Sci.* **27** 148
- Nozières P 1989 *J. Physique* **50** 2541
- Nye J F 1970 *Proc. R. Soc. A* **315** 381
- 1989 *J. Glaciol.* **35** 17–22
- 1991 *J. Cryst. Growth* **113** 465–76
- 1992 *Physics and Chemistry of Ice* ed N Maeno and T Hondoh (Sapporo: Kokkaido University Press) pp 200–5
- Nye J F and Frank F C 1973 *Int. Assoc. Sci. Hydrol. Pub.* **95** 157–61
- O'Neill K and Miller R D 1985 *Water Resources Res.* **21** 281–96
- Ocampo J and Klinger J 1983 *J. Phys. Chem.* **87** 4325

- Offenbacher E L, Roselman I C and Tabor D 1973 *Physics and Chemistry of Ice* ed E Whalley, S J Jones and L W Gold (Ottawa: Royal Society of Canada) pp 377-81
- Ohnesorge R, Löwen H and Wagner H 1991 *Phys. Rev. A* **43** 2870-8
- Oliphant J L and Low P F 1982 *J. Coll. Interface Sci.* **89** 366
- 1983 *J. Coll. Interface Sci.* **95** 45
- Osterkamp T E, Baker G C, Harrison W D and Matava T 1989 *J. Geophys. Res.* **94** (C11) 16227-36
- Overloop K and van Gerven L 1993 *J. Magn. Reson. A* **101** 179-87
- Oxtoby D W 1990 *Nature* **347** 725-30
- Ozawa H and Kinosita S 1989 *J. Coll. Interface Sci.* **132** 113
- Padilla F and Villeneuve J P 1990 *Proc. 5th Canadian Permafrost Conf.* (National Research Council Canada) pp 43-9
- 1992 *Cold Regions Sci. Technol.* **20** 183-94
- Page D L 1972 *Water: A Comprehensive Treatise* vol 1, ed F Franks (New York: Plenum)
- Partanen J I and Lindström M J 1991 *Acta Chem. Scand.* **45** 172-6
- Patterson D E and Smith M W 1980 *Cold Regions Sci. Technol.* **3** 205
- Peixoto J P and Oort A H 1992 *Physics of Climate* (New York: American Institute of Physics)
- Pengra D B and Dash J G 1992 *J. Phys.: Condens. Matter* **4** 7317-32
- Perfect E and Williams P J 1980 *Cold Regions Sci. Technol.* **3** 101
- Permafrost: Fifth International Conference 1988 *Proceedings* (Trondheim, Norway)
- Permafrost: Sixth International Conference 1993 *Proceedings* (Beijing, China)
- Péwé T L 1966 *Permafrost and Its Effect on Life in the North* (Corvallis, OR: Oregon State University Press)
- Phillips J M 1989 *Langmuir* **5** 571-5
- 1990 *Phys. Lett.* **147** 54
- Pietronero L and Tosatti E 1979 *Solid State Commun.* **32** 255-9
- Piper D, Holden J T and Jones R H 1988 *Proc. 5th Int. Conf. on Permafrost* vol 1, ed K Senneset (Trondheim: Tapir) p 370
- Pluis B, denier van der Gon A W, Frenken J W M and van der Veen J F 1987 *Phys. Rev. Lett.* **59** 2678-81
- Pluis B, Taylor T N, Frenkel D and van der Veen J F 1989 *Phys. Rev. B* **40** 1353-6
- Polar Research Board 1984 *Ice Segregation and Frost Heaving* Natl Res Council (Washington, DC: National Academy Press)
- Poole P H, Essmann U, Sciortino S and Stanley H E 1993a *Phys. Rev. E* **48** 3799-3817
- 1993b *Phys. Rev. E* **48** 4605-10
- Prince K C, Breuer U and Bonzel H P 1988 *Phys. Rev. Lett.* **60** 1146-9
- Radd F J and Oertel D H 1973 *2nd Int. Symp. on Permafrost*, Yakutsk p 377
- Rall M, Brison J P and Sullivan N S 1991 *Phys. Rev. B* **44** 9639-42
- Ratke S K, Yamamoto H, Takashi H, Ohrai T and Okamoto J 1982 *Frost i Jord* **24** 22
- Ray R J, Krantz W D, Caine T N and Gunn R D 1983 *J. Glaciol.* **29** 317-37
- Raymond C F and Harrison W D 1975 *J. Glaciol.* **14** 213-33
- Reed M A, Lovell C W, Altschaeffl and Wood L E 1979 *Can. Geotech. J.* **16** 463-72
- Reynolds O 1901 *Papers on Mechanical and Physical Subjects* vol 2 (Cambridge: Cambridge University Press) p 737
- Riecke R D, Vison T S and Mageau D W 1983 *4th Int. Conf. on Permafrost* (Fairbanks: University of Alaska Press) pp 1066-9, 2734-8
- Rong F, Jinsheng Z and Zhongjie H 1983 *4th Int. Conf. on Permafrost* (Fairbanks: University of Alaska Press) pp 311-15
- Sayles F H 1988 *Proc. 5th Int. Symp. on Ground Freezing* vol 1, ed R H Jones and J T Holden (Rotterdam: Balkema) pp 143-65
- Sayward J M 1979 *CRREL Special Report 79-17* (Cold Regions Research and Engineering Laboratory, Hanover, NH)
- Schick M 1990 *Liquids at Interfaces. Les Houches Session XLVIII* ed J Charvolin, J Joanny and J Zinn-Justin (Amsterdam: Elsevier) pp 419-96
- Schick M and Shih W H 1987 *Phys. Rev. B* **35** 5030-5
- Schofield R K 1935 *Trans. 3rd Int. Congr. on Soil Science* vol 2 (Oxford: Oxford University Press) p 37
- Schwertfeger P 1963 *J. Glaciol.* **4** 789-807
- Sei T and Gonda T 1989 *J. Cryst. Growth* **94** 697-707
- Sellman P V, Lewellen R I, Ueda H T, Chamberlain E and Blouin S E 1977 *CRREL Special Report 77-41* (Cold Regions Research and Engineering Laboratory, Hanover, NH)
- Shechter H, Brener R, Folman M and Suzanne J 1990 *Phys. Rev. B* **41** 2748-56
- Shechter H, Brener R and Suzanne J 1988 *Europhys. Lett.* **6** 163-7

- Shimoda M, Misuzaki T, Hiroi M, Hirai A and Eguchi K 1986 *J. Low Temp. Phys.* **64** 285
- Shreve R L 1984 *J. Glaciol.* **30** 341
- Smith M W and Tice A R 1988 *CRREL Report 88-18* (Cold Regions Research and Engineering Laboratory, Hanover, NH) unpublished
- Sommerfeld R A, Mosier A R and Musselman R C 1993 *Nature* **361** 140
- Souchez R A and Lorain R D 1991 *Ice Composition and Glacier Dynamics* (Berlin: Springer)
- Stock K D 1980 *Surf Sci.* **91** 655
- Stock K D and Menzel E 1978 *J. Cryst. Growth* **43** 135
- Strange J H, Rahm M and Smith E G 1993 *Phys. Rev. Lett.* **71** 3589–91
- Stranski I N 1942 *Die Naturwissen.* **28** 425–30
- Taber S 1929 *J. Geol.* **37** 428  
— *J. Geol.* **38** 303
- Takahashi T 1983 *J. Phys. Chem.* **87** 4122–4
- Takahashi T, Ohrai T, Yamamoto H and Okamoto J 1981 *Eng. Geol.* **18** 245
- Takeuchi N, Selloni A and Tosatti E 1994 *Phys. Rev. Lett.* **72** 2227–30
- Tammann G 1910 *Z. Phys. Chem.* **68** 205–8
- Tarazona P and Vicente L 1985 *Mol. Phys.* **56** 557
- Taylor J E, Cahn J W and Handwerker C A 1992 *Acta Metall.* **40** 1443–74
- Tell J L and Maris H J 1983 *Phys. Rev. B* **28** 5122
- Thien Binh V and Melinon P 1985 *Surf Sci.* **161** 234–44
- Thien Binh V, Uzan R and Drechsler M 1978 *J. Physique Lett.* **39** L385–8
- Thompson M E 1991 *J. Geophys. Res.* **B** **96** 4157
- Thomson W 1871 *Phil. Mag.* **42** 448
- Tice A R, Black T R and Berg R L 1988 *CRREL Report 88-19* (Cold Regions Research and Engineering Laboratory, Hanover, NH)
- Tice A R, Burrous C M and Anderson D M 1978 *Proc. 3rd Int. Conf. on Permafrost* vol 1 (Ottawa: National Research Council of Canada) p 149
- Tice A R, Oliphant J L, Nakano Y and Jenkins T F 1982 *CRREL Report 82-15* (Cold Regions Research and Engineering Laboratory, Hanover, NH)
- Tice A R, Zhu Yuanlin and Oliphant J L 1984 *CRREL Report 84-16* (Cold Regions Research and Engineering Laboratory, Hanover, NH)
- Tiller W A 1991 *The Science of Crystallization* vol 1 (Cambridge: Cambridge University Press)
- Timur A 1968 *Geophysics* **33** 584
- Topp G C, Davis J L and Annan A P 1980 *Water Resources Res.* **16** 574–82
- Tourtellotte W W, Rosario I P, Conrad A and Syndulko K 1993 *J. Neural Transmission Suppl.* **39** 5–15
- Trayanov A and Tosatti E 1987 *Phys. Rev. Lett.* **59** 2207
- Trittibach R, Grüter Ch and Bilgram J H 1994 *Phys. Rev. B* **50** 2529–36
- Turnbull D 1952 *J. Chem. Phys.* **20** 411  
— 1956 Solid State Physics *Adv. Res. Appl.* **8** ed F Seitz and D Turnbull (New York: Academic) p 225
- Turner G J and Stow C D 1984 *Phil. Mag.* **49** L25–30
- Tyndall J 1856 *Proc. R. Soc.* **9** 76
- Ubbelohde A R 1965 *Melting and Crystal Structure* (Oxford: Clarendon)
- Untersteiner N 1968 *J. Geophys. Res.* **73** 1251
- Valdez M P and Dawson G A 1989 *J. Geophys. Res.* **94** 1095–103
- Valkealahti S and Nieminen R M 1987 *Phys. Scr.* **36** 646–50
- van der Eerden J P 1993 *J. Cryst. Growth* **128** 62–8
- van der Veen J F, Pluis B and Denier van der Gon A W 1988 *Chemistry and Physics of Solid Surfaces* vol 7, ed R Vanselow R and R F Howe (Berlin: Springer) pp 455–67
- van Loon W K P, Perfect E, Groeneveld P H and Kay B D 1990 *Proc. Int. Symp. on Frozen Soil Impacts on Agricultural, Range, and Forest Lands Spokane, WA* ed K R Cooley (CRREL Special Report 90-1) p 186
- Van Vliet-Lanoe B 1988 *Proc. 5th Int. Conf. on Permafrost* vol 1, ed K Senneset (Trondheim: Tapir) p 1088
- Vialov S S 1965 *Translation 74* (Cold Regions Research and Engineering Laboratory, Hanover, NH) unpublished
- Vignes M and Dijkema K M 1974 *J. Coll. Interface Sci.* **49** 165
- Walder J and Hallet B 1985 *Geol. Soc. Am. Bull.* **96** 336  
— 1986 *Arctic Alpine Res.* **18** 27
- Washburn A L 1973 *Periglacial Processes and Environments* (New York: St Martin's Press)
- 1980 *Geocryology* (New York: Wiley)
- Weber T A and Stillinger F H 1983 *J. Phys. Chem.* **87** 4277

- Weeks J D 1979 *Ordering in Strongly Fluctuating Condensed Matter Systems* ed T Riste (Dordrecht: Reidel) pp 293–318
- 1995 *IAPSO Adv. Study Institute: Physics of Ice-Covered Seas* ed M Leppäranta, in press
- Weeks W F and Ackley S F 1986 *The Geophysics of Sea Ice* ed N Untersteiner (New York: Plenum) pp 9–164
- Wettlaufer J S 1992 *Europhys. Lett.* **19** 337–42
- Wettlaufer J S, Jackson M and Elbaum M 1994 *J. Phys. A: Math. Gen.* **27** 5957–67
- Wettlaufer J S and Weeks W F 1995 *Rev. Geophys.* to be published
- Wettlaufer J S and Worster M G 1994 *Bull. Am. Phys. Soc.* **39** 796
- 1995 *Phys. Rev. E* in press
- Whalley E *et al* 1991 *J. Mol. Struct.* **250** 337–49
- Wiechert H, Lauter H J and Stühn B 1982 *J. Low. Temp. Phys.* **48** 209–15
- Wilen L 1993 Private communication
- Wilen L and Dash J G 1994 *Phys. Rev. Lett.* (submitted)
- Wilen L, Wettlaufer J S, Elbaum M and Schick M 1994 *Phys. Rev. B* (submitted)
- Williams E 1985 *J. Geophys. Res.* **90** 6013–25
- 1988 *Sci. Am.* Nov 88–99
- 1990 *Proc. AMS Conf. on Cloud Physics, San Francisco* pp 282–9
- Williams P J 1986 *Carleton University Press* 2nd edn (Oxford: Oxford University Press) p 137
- Wilson C T R 1929 *J. Franklin Inst.* **208** 1–10
- Wilson R C and Vinson T S 1983 *Transp. Res. Report 83-15* (Corvallis, OR: Oregon State University)
- Wolff E W and Paren J G 1984 *J. Geophys. Res.* **89** 9433–8
- Workman E J and Reynolds S E 1948 *Phys. Rev.* **74** 709–13
- Worster M G 1992 *Interactive Dynamics of Convection and Solidification* ed S H Davis *et al* (Dordrecht: Kluwer)
- Wortis M 1988 *Chemistry and Physics of Solid Surfaces* ed R Vanselow and R F Howe (Berlin: Springer) pp 367–405
- Xia T K, Jian O, Ribarsky M W and Landman U 1992 *Phys. Rev. Lett.* **69** 1967–70
- Xie Y *et al* 1993 *Phys. Rev. Lett.* **71** 2050–3
- Zegelin S J, White I and Jenkins D R 1989 *Water Resources Res.* **25** 2367–76
- Zeppenfeld P, Bienfait M, Liu Feng Chuan, Vilches O E and Coddens G 1990 *J. Physique* **51** 1929–38
- Zhu D M and Dash J G 1986 *Phys. Rev. Lett.* **57** 2959–62
- 1988 *Phys. Rev. Lett.* **60** 432–5